

## Conical extrusion of a work-hardening material: an asymptotic analysis

R.E. JOHNSON

*Department of Theoretical and Applied Mechanics, University of Illinois at Urbana-Champaign,  
216 Talbot Laboratory, 104 South Wright Street, Urbana, IL 61801, USA*

Received 1 June 1987; accepted 11 August 1987

**Abstract.** We study steady-state conical extrusion of an isotropic, power-law hardening material with a Coulomb friction condition present at the die faces. An asymptotic theory is developed based on an axial velocity field which is nearly “slug-like”, i.e., a deformation field for which the transverse variations of the axial velocity are modest in size. However, although the velocity is “slug-like”, within the asymptotic limit considered the shear stresses are not negligible compared to the longitudinal deviatoric stresses. For this reason the theory accounts for the first manifestations of inhomogeneous deformation. In practical terms the validity of the asymptotic theory generally requires either the friction coefficient  $\mu$  to be small or the die slope  $\Delta h/L$  to be small (where  $\Delta h$  is the radius reduction and  $L$  the die length). The primary result of the work is the set of equations (76)–(78). In addition, the present formulation enables for the first time the development of a model of inhomogeneous deformation in conical extrusion which is analogous to the very popular inhomogeneous deformation theory developed by Orowan for plane-strain sheet rolling. Results are presented for a number of examples illustrating the departure from a state of homogeneous compression which is typically found.

### 1. Introduction

Conical extrusion has attracted considerable attention from researchers interested in materials processing for many years. The present paper is an attempt to provide some additional insight into this difficult subject by taking a look at the problem from a slightly different angle using asymptotic methods. The most popular methods of analysis in this subject have been concentrated in three areas: slip-line analysis, upper-bound solutions, and finite-element methods. The number of studies in each of these areas are so numerous that a complete bibliography can not be provided here. However, a few references to help the interested reader get started in the subject include: Collins and Williams [1], Chenot et al. [2], Richmond and Morrison [3], Avitzur [4–7], Osakada and Niimi [8], Lee, Mallett and Yang [9], Lee, Mallett and McMeeking [10], and Kobayashi [11].

We will focus our attention on steady-state extrusion and assume that we have an isotropic work-hardening material wherein the flow stress is proportional to a power of the total plastic strain. We will include elasticity initially, although we will see from the analysis that in the present context its contribution is secondary. Of course to recover residual stresses its effect can not generally be neglected. The analysis will be valid for axisymmetric dies of rather general cross-sectional shape  $\hat{h}(\hat{z})$  where  $\hat{z}$  is the axial position along the die centerline. However, specific calculations will be restricted to conical dies. We will limit ourselves to a friction boundary condition, i.e., Coulomb friction, where the shear stress at the die surface is proportional to the normal stress, but the analysis can be pursued for a much wider range of boundary conditions if desired.

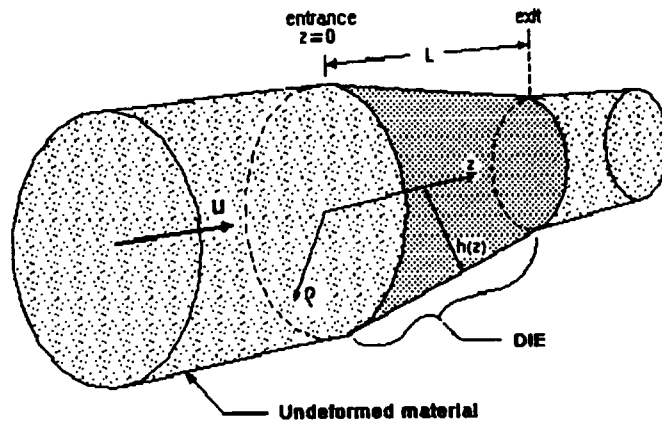


Fig. 1. Schematic of conical extruder.

The goal of the present paper is to develop an approximate theory for the conical extrusion of an isotropic work-hardening material. As we shall see, the key ingredient behind the present approximation is that the axial velocity is nearly one-dimensional with transverse variations appearing at second order, i.e., the flow is a perturbation of a “slug-like” flow. Note, however, that in what follows the shear stresses are generally of the same order of magnitude as the longitudinal deviatoric stresses and consequently the stress field is not necessarily a small perturbation from a state of homogeneous compression. Also note that the transverse variations of the axial velocity field and the deformation of initially plane sections which appear at second order will be evaluated. Admittedly the assumption of a near “slug-like” flow is fairly restrictive and of somewhat limited practical utility, but the results are nonetheless interesting and instructive, and offer a potentially useful simple case against which more elaborate numerical calculations can be tested.

At the heart of the approximation of “slug-like” flow will be the assumption that  $\beta = (\Delta h/L)(\mu\sigma_0/Y_0)$  is small compared to unity;  $\Delta h$  is the change in the die radius from entrance to exit (i.e., the radius reduction),  $L$  is the length of the die,  $\mu$  is the friction coefficient,  $\sigma_0$  is the characteristic pressure (consequently  $\mu\sigma_0$  is the characteristic shear stress) and  $Y_0$  is the characteristic flow stress, i.e., the initial yield stress. The transverse variation of the axial velocity will be shown to be of order  $\beta$  and therefore our restriction requiring  $\beta$  to be small implies a near “slug-like” flow. For convenience we introduce  $\delta = \Delta h/L$  and  $\tau = Y_0/\sigma_0$  and write  $\beta = \delta\mu/\tau$ . In what follows the above assumption will generally be satisfied by  $\delta\mu$  being small compared to unity, since the parameter  $\tau = Y_0/\sigma_0$  is typically of order unity. Physically speaking the flow is “slug-like” either because the slope of the die wall is small (i.e.,  $\delta = \Delta h/L \ll 1$ ), or the friction coefficient  $\mu$  is small, or both are small. From a practical point of view, the friction coefficient  $\mu$  is often rather small and we will see later that for the specific cases examined here the calculations will be restricted to values of  $\mu$  less than about 0.2 (for larger values of  $\mu$  we generally find that the asymptotic theory is not valid). In addition, a further assumption will be made in order to allow us to simplify the friction boundary condition at the die surface, namely, we will assume that the slope of the die wall is sufficiently gentle so that we may neglect terms of order  $\delta^2$  in the stress field. We will, however, compute the contribution to the radial variation in the axial velocity which occurs at this order. We will also find that the cases of most interest, namely those departing furthest

from a state of homogeneous compression, will correspond to  $\mu/\tau = O(1)$  and therefore  $\delta^2$  will necessarily be small since we require  $\beta = \delta\mu/\tau$  to be small.

Within the confines of the asymptotic theory being considered we identify two subcases of practical interest. The first case corresponds to deformation having relatively weak shear stresses, i.e., a perturbation from a state of homogeneous compression. The second and more interesting case alluded to above corresponds to deformations for which the shear stresses have a magnitude comparable to the longitudinal deviatoric stresses and we refer to it as inhomogeneous deformation. The two cases are identified by the magnitude of the parameter  $\mu/\tau = \mu\sigma_0/Y_0$  which is the ratio of the characteristic shear stress to the characteristic flow stress. The case of homogeneous compression corresponds to  $\mu/\tau \ll 1$  and it is found to be valid when the friction coefficient  $\mu$  is sufficiently small so that  $\mu/\ln(1/\mu) \ll \delta$ . The second case of inhomogeneous deformation corresponds to  $\mu/\tau = O(1)$  and it is valid for friction coefficients for which  $\mu/\ln(1/\mu) = O(\delta)$ . The main result of the paper is the set of coupled equations (76)–(78) which determines the normal stress, shear stress and longitudinal deviatoric stress.

As we will see later, within the present formulation for conical extrusion one can identify the counterpart of the popular approximation made by Orowan [12] for inhomogeneous deformation in strip rolling. Using his tremendous insight, Orowan derived an approximate theory for inhomogeneous plane-strain deformation during rolling based on a somewhat ad hoc analogy between rolling deformation and Prandtl's [13] solution for compression of a plastic strip between parallel plates. Unfortunately a similar analogy is not easily made for conical extrusion and consequently, to this author's knowledge, an approximation similar to Orowan's has not been made for conical extrusion. Here we will systematically identify an approximation equivalent to Orowan's, however, because we find that it is based on a somewhat ad hoc assumption we will present only a limited number of results for this case. A separate paper will specifically address the strip-rolling problem using the present approach.

## 2. Formulation

### (a) Governing equations

We begin with the well-known elastic–plastic equations which in dimensional form are given during plastic flow by (in the sequel a caret will denote a dimensional quantity),

$$\hat{D}_{ij} = \frac{1}{2}(\hat{v}_{i,j} + \hat{v}_{j,i}) = \hat{D}_{ij}^p + \hat{D}_{ij}^e, \tag{1}$$

$$\left. \begin{aligned} \hat{d}_{ij}^e &= \hat{D}_{ij}^e - \frac{1}{3}\hat{D}_{kk}^e \delta_{ij} = \frac{1}{2G} \hat{s}_{ij}, \\ \hat{D}_{kk}^e &= \frac{1}{3K} \hat{\sigma}_{kk}, \end{aligned} \right\} \text{(elastic part)} \tag{2}$$

$$\hat{D}_{ij}^p = \lambda \hat{s}_{ij}, \tag{3}$$

$$\left. \begin{aligned} \hat{D}_{ij}^p &= \lambda \hat{s}_{ij}, \\ \hat{D}_{kk}^p &= 0, \end{aligned} \right\} \text{(plastic part)} \tag{4}$$

$$\tag{5}$$

and the equilibrium equations

$$\hat{\sigma}_{ij,j} = 0, \tag{6}$$

understanding that the superscripts *e* and *p* denote the elastic and plastic part, respectively.  $\hat{D}_{ij}$  is the total strain rate,  $\hat{d}_{ij}$  is the deviatoric strain rate,  $\hat{\sigma}_{ij}$  is the total stress,  $\hat{s}_{ij}$  is the deviatoric stress,  $\hat{v}_i$  is the velocity field and  $\hat{v}_{i,j}$  is the velocity gradient matrix.  $\lambda$  is the plastic multiplier and the stress rates  $\dot{\sigma}_{ij}$  and  $\dot{s}_{ij}$  are the Jaumann or corotational stress rates, i.e.,  $\dot{F}_{ij} = \partial F_{ij} / \partial \hat{t} + \hat{v}_k \partial F_{ij} / \partial \hat{x}_k + \hat{\Omega}_{pj} F_{ip} + \hat{\Omega}_{pi} F_{jp}$  where  $\hat{\Omega}_{ij} = \frac{1}{2}(\hat{v}_{i,j} - \hat{v}_{j,i})$  is the vorticity tensor. *G* is the shear modulus, *K* is the bulk modulus and  $\nu$  will be Poisson's ratio. For purely elastic loading or unloading we consider the above equations omitting the plastic terms.

We assume that the flow stress is proportional to a power of the total plastic strain and the flow-rate or yield criterion is

$$\sqrt{\frac{3}{2} \hat{s}_{ij} \hat{s}_{ij}} = Y_0 \left( 1 + \frac{\epsilon_p}{\epsilon_0} \right)^{1/n}, \tag{7}$$

with the total plastic strain  $\epsilon_p$  given by an integral of the plastic strain rate following a material particle, i.e.,

$$\epsilon_p = \int_0^{\hat{t}} \sqrt{\frac{3}{2} \hat{D}_{ij}^p \hat{D}_{ij}^p} d\hat{t}, \tag{8}$$

where  $\hat{t}$  is the time and  $Y_0$  (the initial yield stress),  $\epsilon_0$  and *n* are material parameters. Typical values might place *n* between 5 and 10 and  $\epsilon_0$  in the neighbourhood of 0.01.

The equations are now made dimensionless. We use cylindrical coordinates (*ρ*,  $\phi$ , *z*) and the axial and radial coordinates are made dimensionless using the characteristic lengths in the corresponding directions, i.e., the length of the die *L* and the change in the die radius from entrance to exit  $\Delta h = \hat{h}(0) - \hat{h}(L)$ , respectively,

$$z = \hat{z}/L, \quad \rho = \hat{\rho}/\Delta h. \tag{9}$$

Motivated by mass conservation the required dimensionless form for the velocity components in the axial and radial directions is

$$v_z = \hat{v}_z/U, \quad v_\rho = \hat{v}_\rho/\delta U, \tag{10}$$

where  $\delta = \Delta h/L$  and *U* is the axial velocity of the material entering the die. We also introduce a dimensionless die radius  $q = h(z) = \hat{h}(z)/\Delta h$ .

The deviatoric stresses are of the order of the flow stress of the material and therefore they are made dimensionless using a stress magnitude characteristic of the flow stress (see (7)), i.e.,

$$s_{ij} = \hat{s}_{ij}/Y_0. \tag{11}$$

The total stresses  $\sigma_{ij}$ , however, are made dimensionless by a stress magnitude typical of the pressure in the die. For the time being we will simply denote this characteristic stress by  $\sigma_0$

and write

$$\sigma_{ij} = \hat{\sigma}_{ij}/\sigma_0. \tag{12}$$

Along with this we introduce the parameter  $\tau = Y_0/\sigma_0$ . A specific choice for  $\sigma_0$  will be made later, however one example would be to take  $\sigma_0$  equal to the maximum value of  $|\sigma_{\theta\theta}|$  since we will see that within the context of the present approximation  $-\sigma_{\theta\theta}$  will be equal to the die pressure at leading order.

Time and the plastic multiplier are made dimensionless as follows,

$$t = \hat{t}/(L/U), \quad \lambda = \hat{\lambda}/(U/Y_0L). \tag{13}$$

From (2) a convenient elastic strain rate scale is the stress magnitude  $Y_0$  divided by the shear modulus  $G$  (or bulk modulus) times the characteristic time  $L/U$ . Consequently, the elastic strain rates are made dimensionless as follows,

$$D_{ij}^e = \hat{D}_{ij}^e/(Y_0U/GL). \tag{14}$$

Lastly, we nondimensionalize the plastic strain rates by a characteristic plastic strain rate associated with the flow, namely  $U/L$ ,

$$D_{ij}^p = \hat{D}_{ij}^p/(U/L). \tag{15}$$

Finally the governing equations (1)–(6) for the case of axisymmetric deformation now take on the following dimensionless form; the equilibrium equations,

$$\frac{\partial \sigma_{\theta\theta}}{\partial \varrho} + \delta \tau \frac{\partial s_{\theta z}}{\partial z} + \frac{\sigma_{\theta\theta} - \sigma_{\phi\phi}}{\varrho} = 0, \tag{16}$$

$$\frac{\partial s_{\theta z}}{\partial \varrho} + \frac{\delta}{\tau} \frac{\partial \sigma_{zz}}{\partial z} + \frac{s_{\theta z}}{\varrho} = 0, \tag{17}$$

the strain-rate equations,

$$\frac{\partial v_\varrho}{\partial \varrho} = D_{\theta\theta}^p + \alpha D_{\theta\theta}^e, \quad \frac{v_\varrho}{\varrho} = D_{\phi\phi}^p + \alpha D_{\phi\phi}^e, \tag{18}$$

$$\frac{\partial v_z}{\partial z} = D_{zz}^p + \alpha D_{zz}^e, \tag{19}$$

$$\frac{\partial v_z}{\partial \varrho} + \delta^2 \frac{\partial v_\varrho}{\partial z} = 2\delta (D_{\theta z}^p + \alpha D_{\theta z}^e), \tag{20}$$

(where  $\alpha = Y_0/G$ ), the elastic strain rates,

$$D_{ij}^e - \frac{1}{3} D_{kk}^e \delta_{ij} = \frac{1}{2} \hat{s}_{ij}, \tag{21}$$

$$D_{kk}^e = \frac{1 - 2\nu}{2(1 + \nu)} \frac{\dot{\sigma}_{kk}}{\tau}, \quad (22)$$

the plastic strain rates,

$$D_{ij}^p = \lambda s_{ij}, \quad D_{kk}^p = 0, \quad (23)$$

and the flow-rule,

$$\sqrt{\frac{3}{2}} s_{ij} s_{ij} = \left(1 + \frac{\varepsilon_p}{\varepsilon_0}\right)^{1/n}, \quad \text{where } \varepsilon_p = \int_0^t \sqrt{\frac{2}{3}} D_{ij}^p D_{ij}^p dt. \quad (24)$$

Note that  $\tau = Y_0/\sigma_0$  appears in the above equation due to the different scalings used for  $s_{ij}$  and  $\sigma_{ij}$ , and that  $\alpha = Y_0/G$  is typically of order  $10^{-3}$  and therefore we will assume that it is small.

Using the fact that  $\lambda s_{ij} = D_{ij}^p$  and  $s_{\phi\phi} = -(s_{\theta\theta} + s_{zz})$  we can rewrite the flow-rule as

$$S^2 + s_{\theta\theta}^2 = \frac{1}{3} \left\{ 1 + \frac{2}{\sqrt{3}\varepsilon_0} \int_0^t \lambda \sqrt{S^2 + s_{\theta\theta}^2} dt \right\}^{2/n}, \quad (25)$$

where we define  $S^2 = s_{\theta\theta}^2 + s_{zz}^2 + s_{\theta\theta}s_{zz}$ .

The boundary conditions include the following:

(i) Rigid-body motion of the undeformed material approaching the die. Consequently, the dimensionless axial velocity ahead of the die is unity,

$$v_z = 1, \quad \text{ahead of the die.} \quad (26)$$

(ii) Vanishing normal component of velocity at the impenetrable die faces, i.e.,  $\mathbf{v} \cdot \mathbf{n} = 0$  on  $\varrho = h(z)$ . Using cylindrical coordinates this becomes

$$v_\varrho - v_z \frac{dh}{dz} = 0 \quad \text{on } \varrho = h(z). \quad (27)$$

(iii) A friction boundary condition at the die faces. In particular, we take the shear stress to be proportional to the normal stress with the proportionality constant, i.e., the friction coefficient, taken to be  $\mu$ . This gives

$$\mu \{ \sigma_{\theta\theta} - 2\delta\tau h' s_{\theta z} + \delta^2 h'^2 \sigma_{zz} \} = \tau s_{\theta z} (1 - \delta^2 h'^2) + \delta h' (\sigma_{\theta\theta} - \sigma_{zz}), \quad \text{on } \varrho = h(z), \quad (28)$$

where  $h' = dh/dz$ .

(iv) The remaining condition is a condition on the applied tension in the material after it leaves the die. In extrusion there is generally no net applied tension, however, if we were to consider drawing one would typically have a nonzero applied tension. In the present study

we will restrict our attention to the deformation in the die alone and we will not evaluate the deformation and unloading after the material leaves the die. Therefore we will model the exit condition for extrusion by requiring that there is no net axial force at the exit section of the die, i.e.,

$$2\pi \int_0^{h^{(1)}} \sigma_{zz} \varrho d\varrho = F_{\text{applied}} = 0, \quad \text{at } z = 1. \quad (29)$$

(b) *Asymptotic expansions*

To begin with, we expand the velocity field and strain rates in terms of a small parameter  $\beta$ , which will be identified shortly,

$$\begin{aligned} \mathbf{v} &= \mathbf{v}^{(0)} + \beta \mathbf{v}^{(1)} + \dots, \\ D_{ij}^p &= D_{ij}^{p0} + \beta D_{ij}^{p1} + \dots, \\ D_{ij}^e &= D_{ij}^{e0} + \beta D_{ij}^{e1} + \dots \end{aligned} \quad (30)$$

The equations (18)–(23) therefore become

$$\frac{\partial v_\varrho^{(0)}}{\partial \varrho} + \beta \frac{\partial v_\varrho^{(1)}}{\partial \varrho} + \dots = D_{\varrho\varrho}^{p0} + \beta D_{\varrho\varrho}^{p1} + \alpha D_{\varrho\varrho}^{e0} + \dots, \quad (31)$$

$$\frac{v_\varrho^{(0)}}{\varrho} + \beta \frac{v_\varrho^{(1)}}{\varrho} + \dots = D_{\phi\phi}^{p0} + \beta D_{\phi\phi}^{p1} + \alpha D_{\phi\phi}^{e0} + \dots, \quad (32)$$

$$\frac{\partial v_z^{(0)}}{\partial z} + \beta \frac{\partial v_z^{(1)}}{\partial z} + \dots = D_{zz}^{p0} + \beta D_{zz}^{p1} + \alpha D_{zz}^{e0} + \dots, \quad (33)$$

$$\frac{\partial v_z^{(0)}}{\partial \varrho} + \beta \frac{\partial v_z^{(1)}}{\partial \varrho} + \delta^2 \frac{\partial v_\varrho^{(0)}}{\partial z} + \dots = 2\delta \{ D_{\varrho z}^{p0} + \beta D_{\varrho z}^{p1} + \alpha D_{\varrho z}^{e0} \dots \}, \quad (34)$$

$$D_{ij}^{e0} - \frac{1}{3} D_{kk}^{e0} \delta_{ij} + \beta (D_{ij}^{e1} - \frac{1}{3} D_{kk}^{e1} \delta_{ij}) + \dots = \frac{1}{2} \dot{s}_{ij}, \quad (35)$$

$$D_{kk}^{e0} + \beta D_{kk}^{e1} + \dots = \frac{1 - 2\nu}{2(1 + \nu)} \frac{1}{\tau} \dot{\sigma}_{kk}, \quad (36)$$

$$D_{ij}^{p0} + \beta D_{ij}^{p1} + \dots = \lambda s_{ij}, \quad (37)$$

$$D_{kk}^{p0} + \beta D_{kk}^{p1} + \dots = 0. \quad (38)$$

Turning to the stresses, we expand the normal components of the total and deviatoric stresses in terms of the parameter  $\beta$  as

$$\begin{aligned} s_{ii} &= s_{ii}^{(0)} + \beta s_{ii}^{(1)} + \dots, \\ \sigma_{ii} &= \sigma_{ii}^{(0)} + \beta \sigma_{ii}^{(1)} + \dots, \end{aligned} \quad (39)$$

where  $l = \varrho, z$ , or  $\phi$  and there is no sum on the repeated index here. However, motivated by the friction boundary condition (28) it is convenient to rescale the shear stress as

$$s_{\varrho z} = \frac{\mu}{\tau} \tilde{s}_{\varrho z} = \frac{\mu}{\tau} (\tilde{s}_{\varrho z}^{(0)} + \beta \tilde{s}_{\varrho z}^{(1)} + \dots). \quad (40)$$

This is equivalent to scaling the original dimensional shear stress by  $\mu\sigma_0$ ; i.e.,  $\tilde{s}_{\varrho z} = \hat{s}_{\varrho z}/(\mu\sigma_0)$ . The reason for this rescaling is that it is now apparent that the magnitude of the shear stress is, to a large degree, controlled by the friction boundary condition. With this redefined shear stress the equilibrium equations and leading terms in the friction boundary condition become

$$\frac{\partial \sigma_{\varrho\varrho}}{\partial \varrho} + \mu\delta \frac{\partial \tilde{s}_{\varrho z}}{\partial z} + \frac{\sigma_{\varrho\varrho} - \sigma_{\phi\phi}}{\varrho} = 0, \quad (41a,b)$$

$$\frac{1}{\varrho} \frac{\partial}{\partial \varrho} (\varrho \tilde{s}_{\varrho z}) + \frac{\delta}{\mu} \frac{\partial \sigma_{zz}}{\partial z} = 0,$$

$$\sigma_{\varrho\varrho} - \tilde{s}_{\varrho z} - \frac{\delta}{\mu} h'(\sigma_{\varrho\varrho} - \sigma_{zz}) = O(\mu\delta, \delta^2). \quad (42)$$

In the friction boundary condition the neglect of the omitted terms is consistent with the key assumptions being made in this paper; terms of a similar magnitude in the equilibrium equations will be neglected shortly. Lastly, expanding the plastic multiplier as  $\lambda = \lambda_0 + \beta\lambda_1 + \dots$ , we also have from (23),

$$D_{\varrho\varrho}^{p0} + \beta D_{\varrho\varrho}^{p1} + \dots = \lambda_0 s_{\varrho\varrho}^{(0)} + \beta(\lambda_0 s_{\varrho\varrho}^{(1)} + \lambda_1 s_{\varrho\varrho}^{(0)}) + \dots, \quad (43)$$

$$D_{zz}^{p0} + \beta D_{zz}^{p1} + \dots = \lambda_0 s_{zz}^{(0)} + \beta(\lambda_0 s_{zz}^{(1)} + \lambda_1 s_{zz}^{(0)}) + \dots, \quad (44)$$

$$D_{\phi\phi}^{p0} + \beta D_{\phi\phi}^{p1} + \dots = \lambda_0 s_{\phi\phi}^{(0)} + \beta(\lambda_0 s_{\phi\phi}^{(1)} + \lambda_1 s_{\phi\phi}^{(0)}) + \dots, \quad (45)$$

$$D_{\varrho z}^{p0} + \beta D_{\varrho z}^{p1} + \dots = \lambda_0 \frac{\mu}{\tau} \tilde{s}_{\varrho z}^{(0)} + \beta \frac{\mu}{\tau} (\lambda_0 \tilde{s}_{\varrho z}^{(1)} + \lambda_1 \tilde{s}_{\varrho z}^{(0)}) + \dots \quad (46)$$

From the last of these equations, i.e., equation (46), and equation (34) rewritten here for convenience,

$$\frac{\partial v_z^{(0)}}{\partial \varrho} + \beta \frac{\partial v_z^{(1)}}{\partial \varrho} + \delta^2 \frac{\partial v_z^{(0)}}{\partial z} + \dots = 2\delta(D_{\varrho z}^{p0} + \beta D_{\varrho z}^{p1} + \alpha D_{\varrho z}^{e0} + \dots),$$

we obtain after retaining the leading-order terms

$$\frac{\partial v_z^{(0)}}{\partial \varrho} + \beta \frac{\partial v_z^{(1)}}{\partial \varrho} + \delta^2 \frac{\partial v_z^{(0)}}{\partial z} \simeq 2\delta \frac{\mu}{\tau} \lambda_0 \tilde{s}_{\varrho z}^{(0)} + \dots \quad (47)$$



From this we establish one of the fundamental assumptions of the present theory, namely, we require  $\delta\mu/\tau$  to be small compared to unity and consequently it is appropriate to take

$$\beta = \delta \frac{\mu}{\tau} \ll 1. \tag{48}$$

This clearly amounts to restricting attention to axial velocities which, at leading order, are independent of the radial coordinate, i.e., “slug-like” flows. In addition, in equation (47) note that we will find that the term  $\delta^2 \partial v_\rho^{(0)}/\partial z$  is often small compared to the other three terms retained, however, it is easily retained without incurring any added difficulty.

At leading order we now have from (31)–(34)

$$\frac{\partial v_\rho^{(0)}}{\partial \rho} = D_{\rho\rho}^{p0}, \quad \frac{v_\rho^{(0)}}{\rho} = D_{\phi\phi}^{p0}, \tag{49a,b}$$

$$\frac{\partial v_z^{(0)}}{\partial z} = D_{zz}^{p0}, \tag{50}$$

$$\frac{\partial v_z^{(0)}}{\partial \rho} = 0, \tag{51}$$

and from (51) clearly  $v_z^{(0)}$  will be a function of  $z$  alone. At second order, from (31)–(33) we similarly have

$$\frac{\partial v_\rho^{(1)}}{\partial \rho} = D_{\rho\rho}^{p1} + \frac{\alpha}{\beta} D_{\rho\rho}^{e0}, \quad \frac{v_\rho^{(1)}}{\rho} = D_{\phi\phi}^{p1} + \frac{\alpha}{\beta} D_{\phi\phi}^{e0}, \tag{52}$$

$$\frac{\partial v_z^{(1)}}{\partial z} = D_{zz}^{p1} + \frac{\alpha}{\beta} D_{zz}^{e0}, \tag{53}$$

and from (47) with  $\beta = \delta\mu/\tau$  we have

$$\frac{\partial v_z^{(1)}}{\partial \rho} = 2\lambda_0 \delta_{\rho z}^{(0)} - \frac{\delta^2}{\beta} \frac{\partial v_\rho^{(0)}}{\partial z}. \tag{54}$$

Furthermore, from (31), (32) and (33), equation (38) requiring the trace of the plastic strain rate to vanish gives,

$$\begin{aligned} D_{kk}^{p0} + \beta D_{kk}^{p1} + \dots &= \frac{\partial v_z^{(0)}}{\partial z} + \frac{\partial v_\rho^{(0)}}{\partial \rho} + \frac{v_\rho^{(0)}}{\rho} \\ &+ \beta \left( \frac{\partial v_z^{(1)}}{\partial z} + \frac{\partial v_\rho^{(1)}}{\partial \rho} + \frac{v_\rho^{(1)}}{\rho} - \frac{\alpha}{\beta} D_{kk}^{e0} \right) + \dots = 0, \end{aligned} \tag{55}$$

which at first and second order can be written respectively as

$$\frac{\partial v_z^{(0)}}{\partial z} + \frac{\partial v_\rho^{(0)}}{\partial \rho} + \frac{v_\rho^{(0)}}{\rho} = 0, \quad (56)$$

$$\frac{\partial v_z^{(1)}}{\partial z} + \frac{\partial v_\rho^{(1)}}{\partial \rho} + \frac{v_\rho^{(1)}}{\rho} = \frac{\alpha}{\beta} D_{kk}^{e0} = \frac{1 - 2\nu}{2(1 + \nu)} \frac{\alpha}{\beta \tau} \dot{\sigma}_{kk}, \quad (57)$$

where from (36) we have used

$$D_{kk}^{e0} = \frac{1 - 2\nu}{2(1 + \nu)} \frac{1}{\tau} \dot{\sigma}_{kk}.$$

### 3. Solution

#### (a) Elastic-plastic region

Since we will be interested primarily in the deformation in the plastic region, we begin with a consideration of the solution in this region. From (51) we find that the axial velocity is independent of the radial coordinates at leading order and hence it is a function only of  $z$ ,

$$v_z^{(0)} = v_z^{(0)}(z). \quad (58)$$

The radial component of viscosity is found in terms of the axial component by integrating (56) to find

$$v_\rho^{(0)} = -\frac{\rho}{2} \frac{dv_z^{(0)}}{dz}, \quad (59)$$

where we have used the symmetry condition on the centerline that  $v_\rho(0, z) = 0$ . A radial variation in the axial velocity enters at next order and is ultimately determined from (54) which gives

$$\frac{\partial v_z^{(1)}}{\partial \rho} = 2\lambda_0 \tilde{s}_{\rho z}^{(0)} - \frac{\delta^2}{\beta} \frac{\partial v_\rho^{(0)}}{\partial z} = 2 \frac{\tilde{s}_{\rho z}^{(0)}}{s_{zz}^{(0)}} \frac{dv_z^{(0)}}{dz} + \frac{\delta^2}{\beta} \frac{\rho}{2} \frac{d^2 v_z^{(0)}}{dz^2}. \quad (60)$$

where from (50) and (44) we have used  $\lambda_0 = (dv_z^{(0)}/dz)/s_{zz}^{(0)}$  and we have also used (59) for  $v_\rho^{(0)}$ .

From the boundary condition on the velocity field at the die surface  $\rho = h(z)$  we have at leading order

$$v_\rho^{(0)} - h' v_z^{(0)} = 0, \quad \text{on } \rho = h(z),$$

or using (59)

$$\frac{d(h^2 v_z^{(0)})}{dz} = 0.$$

Consequently,

$$v_z^{(0)} = C/h^2(z) = h^2(0)/h^2(z). \quad (61)$$

where  $C$  is a constant which is easily found to equal  $h^2(0)$  in order to satisfy mass conservation, i.e., the net dimensionless mass flow rate through the die is equal to  $h^2(0)$ . Using (61) the transverse variation in the axial velocity obtained from (60) for a conical extruder ( $h' = 0$ ) becomes

$$\frac{\partial v_z^{(1)}}{\partial \varrho} = -\frac{4h^2(0)h'}{h^3} \left( \frac{\tilde{s}_{\varrho z}^{(0)}}{s_{zz}^{(0)}} - \frac{3}{4} \frac{\tau}{\mu} \frac{\delta h'}{h} \varrho \right). \quad (62)$$

From expression (59) for  $v_\varrho^{(0)}$  we now see that  $\partial v_\varrho^{(0)}/\partial \varrho = v_\varrho^{(0)}/\varrho$  and therefore from (49)  $D_{\varrho\varrho}^{p0} = D_{\phi\phi}^{p0}$  giving from (43) and (45)

$$s_{\varrho\varrho}^{(0)} = s_{\phi\phi}^{(0)} \quad \text{and therefore} \quad \sigma_{\varrho\varrho}^{(0)} = \sigma_{\phi\phi}^{(0)}. \quad (63)$$

Recalling that we have  $s_{\phi\phi} = -(s_{zz} + s_{\varrho\varrho})$  and since we found  $s_{\varrho\varrho}^{(0)} = s_{\phi\phi}^{(0)}$  we have

$$s_{zz}^{(0)} = -2s_{\varrho\varrho}^{(0)}. \quad (64)$$

Using (63), i.e.,  $\sigma_{\varrho\varrho}^{(0)} = \sigma_{\phi\phi}^{(0)}$ , the equilibrium equations become

$$\frac{\partial \sigma_{\varrho\varrho}^{(0)}}{\partial \varrho} + \beta \left( \frac{\partial \sigma_{\varrho\varrho}^{(1)}}{\partial \varrho} + \frac{\sigma_{\varrho\varrho}^{(1)} - \sigma_{\phi\phi}^{(1)}}{\varrho} \right) + \mu \delta \frac{\partial \tilde{s}_{\varrho z}^{(0)}}{\partial z} + \dots = 0, \quad (65a,b)$$

$$\frac{1}{\varrho} \frac{\partial}{\partial \varrho} (\varrho \tilde{s}_{\varrho z}^{(0)}) + \frac{\delta}{\mu} \frac{\partial \sigma_{zz}^{(0)}}{\partial z} + \beta \left( \frac{1}{\varrho} \frac{\partial}{\partial \varrho} (\varrho \tilde{s}_{\varrho z}^{(1)}) + \frac{\delta}{\mu} \frac{\partial \sigma_{zz}^{(1)}}{\partial z} \right) + \dots = 0.$$

In addition, (63) allows us to write

$$\sigma_{zz}^{(0)} = \sigma_{\varrho\varrho}^{(0)} + \frac{3}{2} \tau s_{zz}^{(0)}. \quad (66)$$

Therefore, at leading order the governing equilibrium equations become

$$\frac{\partial \sigma_{\varrho\varrho}^{(0)}}{\partial \varrho} = 0, \quad (67)$$

$$\frac{1}{\varrho} \frac{\partial}{\partial \varrho} (\varrho \tilde{s}_{\varrho z}^{(0)}) = -\frac{\delta}{\mu} \frac{\partial \sigma_{zz}^{(0)}}{\partial z} = -\frac{\delta}{\mu} \left( \frac{\partial \sigma_{\varrho\varrho}^{(0)}}{\partial z} + \frac{3}{2} \tau \frac{\partial s_{zz}^{(0)}}{\partial z} \right). \quad (68)$$

Note that the radial equilibrium equation (67) has undergone considerable simplification and that the axial equilibrium equation (68) has been essentially unaltered preserving a balance between axial stress and shear stress. As we will see soon, axial derivatives are generally of  $O(\mu/\delta)$  and therefore the terms on the right side of (68) are  $O(1)$  and must be retained.

We now see from (67) that at leading order the total radial stress does not vary in the cross section plane, but is a function only of axial position,

$$\sigma_{\varrho\varrho}^{(0)} = \sigma_{\varrho\varrho}^{(0)}(z). \quad (69)$$

From the second equilibrium equation we can write the shear stress as

$$\tilde{s}_{\varrho z}^{(0)} = -\frac{\delta}{\mu} \frac{\varrho}{2} \frac{d\sigma_{\varrho\varrho}^{(0)}}{dz} - \frac{3}{2} \frac{\delta}{\mu} \frac{\tau}{\varrho} \int_0^{\varrho} \varrho' \frac{\partial s_{zz}^{(0)}}{\partial z} d\varrho'. \quad (70)$$

The friction condition (42) on the die faces  $\varrho = h(z)$  can be written using (66) as

$$\tilde{s}_{\varrho z}^{(0)} = \sigma_{\varrho\varrho}^{(0)} + \frac{3}{2} \frac{\delta}{\mu} h' \tau s_{zz}^{(0)}, \quad (71)$$

and substituting for the shear stress from (70) we obtain an equation for  $\sigma_{\varrho\varrho}^{(0)}$  in terms of  $s_{zz}^{(0)}$

$$\frac{d\sigma_{\varrho\varrho}^{(0)}}{dz} + \frac{2\mu}{\delta h(z)} \sigma_{\varrho\varrho}^{(0)} = -\frac{3\tau}{h^2} \frac{d}{dz} \int_0^{h(z)} \varrho s_{zz}^{(0)} d\varrho. \quad (72)$$

For a balance in this equation we now observe the previously stated point that axial derivatives are generally of order  $\mu/\delta$ .

The remaining task is to obtain the leading-order terms in the flow-rule. From (64) we have to leading order  $S^2 = \frac{3}{4} s_{zz}^{(0)2}$  (see (25)) and since from (44) and (46)  $\lambda_0 = D_{zz}^{p0}/s_{zz}^{(0)}$  and  $D_{\varrho z}^{p0} = \lambda_0(\mu/\tau)\tilde{s}_{\varrho z}^{(0)}$ , equation (25) becomes at leading order

$$\frac{3}{4} s_{zz}^{(0)2} + \left(\frac{\mu}{\tau}\right)^2 \tilde{s}_{\varrho z}^{(0)2} = \frac{1}{3} \left\{ 1 + \frac{2}{\sqrt{3}} \frac{1}{\varepsilon_0} \int_0^t D_{zz}^{p0} \left[ \frac{3}{4} + \left(\frac{\mu \tilde{s}_{\varrho z}^{(0)}}{\tau s_{zz}^{(0)}}\right)^2 \right]^{1/2} dt \right\}^{2/n}. \quad (73)$$

We also have from (50)  $D_{zz}^{p0} = dv_z^{(0)}/dz$  giving

$$s_{zz}^{(0)2} + \frac{4}{3} \left(\frac{\mu}{\tau}\right)^2 \tilde{s}_{\varrho z}^{(0)2} = \frac{4}{9} \left\{ 1 + \frac{1}{\varepsilon_0} \int_0^t \frac{dv_z^{(0)}}{dz} \left[ 1 + \frac{4}{3} \left(\frac{\mu \tilde{s}_{\varrho z}^{(0)}}{\tau s_{zz}^{(0)}}\right)^2 \right]^{1/2} dt \right\}^{2/n}. \quad (74)$$

Lastly, it is convenient in this steady-state problem to change integration variables from  $t$  to  $z$ . Consequently, using  $dz/dt \approx v_z^{(0)}$  and  $v_z^{(0)} = h^2(0)/h^2(z)$  the integral following a material particle (given by the streamlines  $\varrho/h(z) = \text{constant}$  at leading order) can be written to leading order as

$$s_{zz}^{(0)2} + \frac{4}{3} \left(\frac{\mu}{\tau}\right)^2 \tilde{s}_{\varrho z}^{(0)2} = \frac{4}{9} \left\{ 1 - \frac{2}{\varepsilon_0} \int_0^z \frac{h'}{h} \left[ 1 + \frac{4}{3} \left(\frac{\mu \tilde{s}_{\varrho z}^{(0)}}{\tau s_{zz}^{(0)}}\right)^2 \right]^{1/2} dz \right\}^{2/n}. \quad (75)$$

In summary, we now have the three coupled equations for the three unknowns  $\sigma_{\varrho\varrho}^{(0)}(z)$ ,  $\tilde{s}_{\varrho z}^{(0)}$ , and  $s_{zz}^{(0)}$ ,

$$\frac{d\sigma_{\varrho\varrho}^{(0)}}{dz} + \frac{2\mu}{\delta h(z)} \sigma_{\varrho\varrho}^{(0)} = -\frac{3\tau}{h^2} \frac{d}{dz} \int_0^h \varrho s_{zz}^{(0)} d\varrho, \quad (76)$$

$$\bar{s}_{\varrho z}^{(0)} = \left( \sigma_{\varrho\varrho}^{(0)} + \frac{3}{2} \frac{\delta}{\mu} \tau h' s_{zz}^{(0)} \right) \frac{\varrho}{h} + \frac{3}{2} \frac{\delta}{\mu} \frac{\tau}{\varrho} \left\{ \left( \frac{\varrho}{h} \right)^2 \int_0^h \varrho \frac{\partial s_{zz}^{(0)}}{\partial z} d\varrho - \int_0^{\varrho} \varrho \frac{\partial s_{zz}^{(0)}}{\partial z} d\varrho \right\}, \quad (77)$$

$$s_{zz}^{(0)2} + \frac{4}{3} \left( \frac{\mu}{\tau} \right)^2 \bar{s}_{\varrho z}^{(0)2} = \frac{4}{9} \left\{ 1 - \frac{2}{\varepsilon_0} \int_0^z \frac{h'}{h} \left[ 1 + \frac{4}{3} \left( \frac{\mu \bar{s}_{\varrho z}^{(0)}}{\tau s_{zz}^{(0)}} \right)^2 \right]^{1/2} dz \right\}^{2/n}. \quad (78)$$

Equation (77) for the shear stress was obtained by rewriting equation (70) using  $d\sigma_{\varrho\varrho}^{(0)}/dz$  obtained from (76). Note that (78) is evaluated following a material particle, i.e.,  $\varrho/h(z) = \text{constant}$ .

The one boundary condition that remains to be satisfied is the requirement that the exit tension is zero, i.e., equation (29). Since  $\sigma_{zz}^{(0)} = \sigma_{\varrho\varrho}^{(0)} + \frac{3}{2} \tau s_{zz}^{(0)}$ , this condition can be written to leading order as

$$\sigma_{\varrho\varrho}^{(0)}(z=1) = -\frac{3\tau}{h^2(1)} \int_0^{h(1)} \varrho s_{zz}^{(0)}(\varrho, 1) d\varrho, \quad (79)$$

which is a condition relating the exit values of  $\sigma_{\varrho\varrho}^{(0)}$  and  $s_{zz}^{(0)}$ .

The only other information required to complete the problem is to determine where the plastic flow first begins, i.e., we must determine the boundary separating the region which is deforming purely elastically from the region of elastic-plastic deformation. We will refer to this boundary as the elastic-plastic boundary. To determine this boundary it is necessary to construct the solution in the neighborhood of the die entrance where the material is deforming elastically. This is done in Appendix I and the key result is that the elastic-plastic boundary is only a small perturbation from the entrance plane of the die  $z = 0$ . This result is easily anticipated and follows from the assumption that  $\alpha = Y_0/G$  is very small. Consequently, equations (76)–(78) are solved in the region  $0 \leq z \leq 1$ .

This completes the leading-order problem for the region which is deforming plastically. Note that elastic effects begin to enter the picture at higher order through equation (57). Namely the leading-order stress field appears as a volume source/sink-like term on the right side of (57), i.e.,

$$\nabla \cdot \mathbf{v}^{(1)} = \frac{1 - 2\nu}{2(1 + \nu)} \frac{\alpha}{\beta\tau} \dot{\sigma}_{kk}^{(0)}. \quad (80)$$

Since  $v_z^{(1)}$  is essentially known from integrating (54), equation (80) then allows the determination of  $v_\varrho^{(1)}$  and the methodology can be pursued further to determine the corresponding modification to the stresses. This elastic effect, however, is generally very small since  $\alpha$  is typically of  $O(10^{-3})$  and therefore the merit in presenting it is questionable. (Note that inherent in the formulation is the assumption that  $\alpha \leq O(\beta)$ ).

#### 4. Results and discussion

The deformation in the plastically deforming region is determined at leading order by solving equations (76)–(78). If we take the characteristic stress  $\sigma_0$  to be equal to  $|\dot{\sigma}_{\varrho\varrho}^{(0)}|$  at the entrance

$z = 0$ , then the dimensionless stress  $\sigma_{\varrho\varrho}^{(0)}(0) = -1$ . Using this and integrating (76) we find  $\sigma_{\varrho\varrho}^{(0)}$  in terms of  $s_{zz}^{(0)}$ ,

$$\sigma_{\varrho\varrho}^{(0)}(z) = e^{-(\mu/\delta)H(z)} \left\{ -1 - 3\tau \int_0^z \left[ \frac{\exp([\mu/\delta]H(z))}{h^2(z)} \frac{d}{dz} \int_0^{h(z)} \varrho s_{zz}^{(0)} d\varrho \right] dz \right\}, \quad (81)$$

where

$$H(z) = 2 \int_0^z \frac{dz}{h(z)}.$$

Note that the characteristic pressure  $\sigma_0 = |\hat{\sigma}_{\varrho\varrho}^{(0)}|$  was a convenient choice since it gives  $\sigma_{\varrho\varrho}^{(0)}(0) = -1$ , but that its value is actually unknown. This is reflected in the fact that boundary condition (80) now really represents an equation for  $\tau = Y_0/\sigma_0$  or equivalently  $\sigma_0$ . It is also beneficial to differentiate the flow-rule (78) and write it as

$$\frac{ds_{zz}^{(0)3}}{dz} + 2 \left( \frac{\mu}{\tau} \right)^2 s_{zz}^{(0)} \frac{d\tilde{s}_{\varrho z}^{(0)2}}{dz} = - \frac{16h'}{9n\varepsilon_0 h} \left\{ \left[ s_{zz}^{(0)2} + \frac{4}{3} \left( \frac{\mu}{\tau} \tilde{s}_{\varrho z}^{(0)2} \right)^2 \right] / (2/3) \right\}^{(3-n)/2}, \quad (82)$$

where the derivative  $d/dz$  is a material or total derivative along the particle pathline or streamline  $\varrho = \varrho(z)$  which to leading order is given by  $\varrho/h(z) = \text{constant}$  since  $v_z^{(0)} = h^2(0)/h^2(z)$ .

An examination of the flow-rule (82) or (78) shows that the parameter  $\mu/\tau$  multiplying the terms involving the shear stress controls much of the character of the solution. Recall that  $\mu/\tau$  is the ratio of the characteristic shear stress and the characteristic yield stress  $\mu\sigma_0/Y_0$  and therefore two limiting cases of practical interest include: (a)  $\mu/\tau \ll 1$ , corresponding to weak shear stress and deformation which is a perturbation of homogeneous compression, and (b)  $\mu/\tau = O(1)$ , which results in a significant shear effect and inhomogeneous deformation. Remembering that the assumption of a ‘‘slug-like’’ flow requires  $\delta\mu/\tau \ll 1$ , we see here that case (a) which essentially corresponds to very small  $\mu$  will be valid for a wide range of die wall slopes  $\delta$ . However, case (b) which has a substantial shear effect will be restricted to rather gentle die slopes, i.e.,  $\delta < O(1)$ , in order to satisfy the axial velocity condition  $\delta\mu/\tau < O(1)$  when  $\mu/\tau = O(1)$ . Case (b) is clearly the case of most interest here and it is not too suprising that the die wall slope must be moderately gentle in order to have a ‘‘slug-like’’ flow even though there are significant shear stresses present. Note that if the statement  $\mu/\tau = O(1)$  is taken at face value, namely that shear effects are important only when  $\mu/\tau$  is strictly of order unity, it would be tempting to neglect the terms involving  $s_{zz}^{(0)}$  in equation (77) for  $\tilde{s}_{\varrho z}^{(0)}$ . This is because the coefficient of these terms is  $\delta/(\mu/\tau)$  and we have required  $\delta$  to be small in order to establish a ‘‘slug-like’’ flow in this situation (recall that we require  $\delta\mu/\tau < O(1)$ ). However, as a practical matter we find that shear stresses begin to play an important role at values of  $\mu/\tau$  which are actually rather modest in magnitude (see the examples discussed below) and consequently we find that  $\delta/(\mu/\tau)$  is not negligible when the shear stress becomes important. In fact, we find that the terms involving  $s_{zz}^{(0)}$  in equation (77) often contribute 30% or more to the total value of the shear stress (this point will be illustrated later in figure 11). With regard to this general point, one must keep in mind that equations (76)–(78) are actually valid for  $\mu/\tau \leq O(1)$  and only when this parameter becomes

very small do we attain a state of homogeneous compression. One can, however, base an ad hoc theory on the omission of the terms involving  $s_{zz}^{(0)}$  in equation (77) for the shear stress and obtain considerable simplification at the expense of a loss of accuracy. Such a theory is related to a popular approximation made in sheet rolling analysis and it will be discussed in section (c) below. A possible third case of interest for which  $\mu/\tau$  is large does not seem to be of practical significance partly because  $\mu$  is typically rather small and therefore  $\mu/\tau$  rarely seems to be large, and also because if  $\mu/\tau$  is large, it is difficult for the “slug-flow” condition  $\delta\mu/\tau \ll 1$  to be satisfied for cases of practical interest.

The specific distinguished limit relevant for the two cases discussed above can be identified more clearly when one realizes that  $\tau$  is actually a function of  $\mu$  and  $\delta$ . The fact that  $\tau$  is related to  $\mu$  and  $\delta$  follows from the fact that  $\tau = Y_0/\sigma_0$  involves  $\sigma_0$  (the characteristic pressure taken here to be  $|\hat{\sigma}_{\varrho\varrho}^{(0)}(0)|$ ) which is actually determined as part of the solution and correspondingly depends on  $\mu$  and  $\delta$ . This becomes clear when we apply the exit stress condition (79) and rewrite it to obtain an expression for  $\tau$  in terms of  $\sigma_{\varrho\varrho}^{(0)}(1)$  and  $s_{zz}^{(0)}$ ,

$$\tau = - \frac{h^2(1)\sigma_{\varrho\varrho}^{(0)}(1)}{3 \int_0^{h(1)} \varrho s_{zz}^{(0)}(\varrho, 1) d\varrho}. \tag{83}$$

Clearly from (81) and (82) we see that  $\sigma_{\varrho\varrho}^{(0)}(1)$  and  $s_{zz}^{(0)}(\varrho, 1)$  depend on  $\mu$  and  $\delta$  and therefore  $\tau$  is a function of  $\mu$  and  $\delta$ . The dependence of  $\tau$  on  $\mu$  and  $\delta$  can, however, be identified a little more precisely as follows. Since the pressure or  $-\sigma_{\varrho\varrho}^{(0)}$  is exponentially decreasing from the entrance to the exit and  $s_{zz}^{(0)}$  is an  $O(1)$  quantity, (83) together with (81) lead us to the result that  $-\sigma_{\varrho\varrho}^{(0)}(1) = O(e^{-\mu/\delta})$  and  $\tau = O(e^{-\mu/\delta})$ . This now enables us to isolate the magnitude of the friction coefficient in terms of  $\delta$  for the two cases of interest, namely  $\mu/\tau \ll 1$  and  $\mu/\tau = O(1)$ . Since we can now write  $\mu/\tau = O(\mu e^{-\mu/\delta})$ , case (a) corresponding to homogeneous compression (valid when  $\mu/\tau \ll 1$ ) gives  $\mu/\ln(1/\mu) \ll O(\delta)$  and case (b) corresponding to inhomogeneous deformation and a significant shear effect occurs when  $\mu/\tau = O(1)$  giving  $\mu/\ln(1/\mu) = O(\delta)$ .

(a) Homogeneous compression

In the first case of homogeneous compression the solution is readily obtained. If we neglect terms of order  $(\mu/\tau)^2$  in the flow-rule (82) and integrate, we find the well-known result for  $s_{zz}^{(0)}$ , i.e.,

$$s_{zz}^{(0)} = \frac{2}{3} \left\{ 1 - \frac{2}{\varepsilon_0} \ln(h) \right\}^{1/n}. \tag{84}$$

Since  $s_{zz}^{(0)}$  is a function only of  $z$  (81) becomes

$$\sigma_{\varrho\varrho}^{(0)} = e^{-(\mu/\delta)H(z)} \left\{ -1 - 3\tau \int_0^z \left[ \frac{\exp((\mu/\delta)H)}{2h^2} \frac{d}{dz} (s_{zz}^{(0)} h^2) \right] dz \right\}. \tag{85}$$

Lastly, using  $\sigma_{\varrho\varrho}^{(0)}$  and  $s_{zz}^{(0)}$  we find the shear stress from (77),

$$s_{\varrho z}^{(0)} = \left( \sigma_{\varrho\varrho}^{(0)} + \frac{3}{2} \frac{\delta}{\mu} \tau h' s_{zz}^{(0)} \right) \frac{\varrho}{h}. \tag{86}$$

(b) *Inhomogeneous deformation*

The case of most interest here is case (b) which has a significant shear effect. In this case it is necessary to resort to numerical techniques to obtain the solution to (76)–(78). The approach taken was to use an initial guess for the stresses and then to iterate on the three equations to find the solution. The initial guess was based on a curve-crawling scheme started with solutions for small  $\mu$ , which were naturally close to homogeneous compression. The scheme then crawled to larger values of  $\mu$  using the previous solution as the first guess for a new value of  $\mu$ . The iteration scheme proceeded as follows: for a known  $\tilde{s}_{zz}^{(0)}$  equation (82) was solved for  $s_{zz}^{(0)}$  using a fourth-order Runge–Kutta scheme on each material pathline of interest. The stress  $\sigma_{\theta\theta}^{(0)}$  was then determined from (81) and substituted along with  $s_{zz}^{(0)}$  into (77) to find a new  $\tilde{s}_{zz}^{(0)}$ . At this point another iteration is started. A summary of the iteration scheme is given below in equations (87)–(89). Omitting the superscript (0) which denotes the leading-order solution and writing instead  $\tilde{s}_{zz}^{(0)} = \tilde{s}_{zz}^k$ ,  $s_{zz}^{(0)} = s_{zz}^k$ , and  $\sigma_{\theta\theta}^{(0)} = \sigma_{\theta\theta}^k$  where the superscript  $k$  indicates the  $k$ th iterate, we have

$$\frac{d(s_{zz}^k)^3}{dz} + 2 \left(\frac{\mu}{\tau}\right)^2 s_{zz}^k \frac{d(\tilde{s}_{zz}^k)^2}{dz} = \frac{16h'}{9n\epsilon_0 h} \left\{ \left[ (s_{zz}^k)^2 + \frac{4}{3} \left(\frac{\mu}{\tau} \tilde{s}_{zz}^k\right)^2 \right] / (2/3) \right\}^{(3-n)/2}, \quad (87)$$

$$\sigma_{\theta\theta}^k = e^{-(\mu/\delta)H} \left\{ -1 - 3\tau \int_0^z \left[ \frac{\exp([\mu/\delta]H)}{h^2} \frac{d}{dz} \int_0^h \varrho s_{zz}^k d\varrho \right] dz \right\}, \quad (88)$$

$$\tilde{s}_{zz}^{k+1} = \left[ \sigma_{\theta\theta}^k + \frac{3}{2} \frac{\delta}{\mu} \tau h' s_{zz}^k \right] \frac{\varrho}{h} + \frac{3}{2} \frac{\delta}{\mu} \frac{\tau}{\varrho} \left\{ \left(\frac{\varrho}{h}\right)^2 \int_0^h \varrho \frac{\partial s_{zz}^k}{\partial z} d\varrho - \int_0^e \varrho \frac{\partial s_{zz}^k}{\partial z} d\varrho \right\}. \quad (89)$$

Note that the last equation involves mixed-order iterates, i.e., it computes the required value of the shear stress based on  $s_{zz}^k$  and  $\sigma_{\theta\theta}^k$  where these quantities were computed with a previous value of the shear stress. Therefore the residual or error to monitor in evaluating the accuracy of the final solution is the quantity  $\tilde{s}_{zz}^{k+1} - \tilde{s}_{zz}^k$  which is conveniently normalized by the local value of the yield stress. The iteration scheme was terminated when this residual was less than  $10^{-3}$  and this typically occurred within fifty iterations. The die was divided into twenty segments (21 nodes) from centerline to the die wall and forty segments (41 nodes) from entrance to exit.

The results which will be discussed in detail shortly show that as  $\mu$  is increased the shear stress at the die faces naturally increases and the magnitude of  $s_{zz}^{(0)}$  decreases. The place where this is most severe is at the die surface right at the entrance, i.e., at  $q = h(0)$ . Recalling that the theory is based on  $v_z \simeq v_z^{(0)}(z)$  and that this requires the term  $\tilde{s}_{zz}^{(0)}/s_{zz}^{(0)} \leq O(1)$  (see equation (60)), we see that the basic theory fails when  $s_{zz}^{(0)}$  becomes sufficiently small such that  $\beta v_z^{(1)}$  becomes comparable in size to  $v_z^{(0)}$ . Consequently, no solution exists within the scope of the present theory above some maximum value of  $\mu$  which depends on the values of the other parameters in the problem. This breakdown of the approximation was manifest in the numerical scheme which required an increasing number of iterations and eventually did not converge as  $\mu$  was increased further. One place where the source of the difficulty in the numerical scheme is easily identified is in the appearance of a term  $1/s_{zz}^{(0)}$  (the origins of which stem from hardening due to shear strain) on the right-hand side of the yield condition (78). In practice, as  $\mu$  gets large and  $s_{zz}^{(0)}$  becomes small, the derivatives with respect to  $z$  become



large near the entrance where the shear is largest and obtaining a converged solution becomes increasingly difficult. For the specific cases, failure of the present approximation and violation of the near “slug-flow” requirement occurred at values of  $\mu$  between 0.10 and 0.20. The rate of convergence for values of  $\mu$  approaching the point where  $s_{zz}^{(0)}$  begins to get small was generally improved by underrelaxing on the shear stress in the iterative procedure.

(c) *An approximate model*

Returning to equations (76)–(78) it is interesting to extract from these equations a greatly simplified ad hoc model or approximation which has a direct analogy with a popular approximate theory frequently used in plane-strain sheet rolling. The approximate theory in sheet rolling to which we are referring is the inhomogeneous theory due to Orowan [12]. For a recent application of this theory, see Venter and Abd-Rabbo [14]. Orowan derived his approximate theory for inhomogeneous deformation by drawing a somewhat ad hoc analogy between the stress field present in rolling with that found by Prandtl [13] for a plastic strip being compressed between parallel plates. The ad hoc nature of this formulation has been previously pointed out by Alexander [15]. Within the framework of the present formulation an approximation exactly equivalent to Orowan’s, but found in a very different way, can be obtained as follows: the coupling between  $\tilde{s}_{\rho z}^{(0)}$  and  $s_{zz}^{(0)}$  in equation (77) is omitted by discarding the terms involving  $s_{zz}^{(0)}$  in (77) so that  $\tilde{s}_{\rho z}^{(0)}$  is approximated by  $\sigma_{\rho\rho}^{(0)}(z)\rho/h$ . The result  $\tilde{s}_{\rho z}^{(0)} \simeq \sigma_{\rho\rho}^{(0)}\rho/h$  is then substituted into the left hand side of the flow-rule equation (78). The term involving the shear stress within the integral on the right-hand side of (78), however, is either omitted so that the integral can be computed explicitly (the value of the flow stress or current yield stress for homogeneous compression), or an expression for the flow stress is prescribed. In either case we have the following approximation for (78),

$$s_{zz}^{(0)2} + \frac{4}{3} \left(\frac{\mu}{\tau}\right)^2 \tilde{s}_{\rho z}^{(0)2} = y^2(z),$$

$$s_{zz}^{(0)} = \sqrt{y^2(z) - \frac{4}{3} \left(\frac{\mu}{\tau} \sigma_{\rho\rho}^{(0)}(z) \frac{\rho}{h}\right)^2}, \tag{90}$$

where  $y(z)$  is a known function, e.g., the right-hand side of equation (78) omitting the term  $(\mu\tilde{s}_{\rho z}^{(0)}/\tau s_{zz}^{(0)})^2$ . Equation (90) can now be substituted into the right-hand side of (76) and the integral can be evaluated, i.e.,

$$\int_0^h \rho s_{zz}^{(0)} d\rho = y(z) \int_0^h \rho \sqrt{1 - \frac{1}{3} a^2 (\rho/h)^2} d\rho = \frac{yh^2}{3a^2} [1 - (1 - a^2)^{3/2}] = yh^2 \omega(a), \tag{91}$$

where

$$a = 2 \frac{\mu}{\tau} \frac{\sigma_{\rho\rho}^{(0)}(z)}{y(z)}$$

and we define a function  $\omega(a) = [1 - (-a^2)^{3/2}]/3a^2$  analogous to the inhomogeneity function introduced by Orowan. Lastly using (91), (76) now becomes a nonlinear ordinary differential equation for  $\sigma_{\theta\theta}^{(0)}$  which we rewrite in more familiar terms as

$$\frac{d}{dz} \{(\delta h)^2 [\sigma_{\theta\theta}^{(0)} + 3\tau y \omega(a)]\} - \delta^2 \frac{dh^2}{dz} \sigma_{\theta\theta}^{(0)} + 2\delta h \mu \sigma_{\theta\theta} = 0. \quad (92)$$

This equation is analogous to the equation for the roll pressure in classical rolling theory. Note that  $-\sigma_{\theta\theta}^{(0)}$  is approximately equal to the roll pressure and  $\mu\sigma_{\theta\theta}$  appearing in the last term above is the approximate shear stress at the die surfaces. There has clearly been an enormous reduction in the complexity of the mathematical problem, since we now have the single equation (92) to solve to complete the solution.

The simplification described above associated with the Orowan approximation introduces one well-known predicament concerning the stress boundary conditions. Namely, under the present circumstances where we have effectively decoupled the equations it is quite possible for the shear stress at the die walls  $\rho = h$  to exceed the local yield stress in shear, i.e.,  $s_{\rho z}^{(0)} \simeq (\mu/\tau) \sigma_{\theta\theta}^{(0)}$  can exceed the limiting value  $(\sqrt{3}/2)y(z)$ . This is a consequence of omitting the terms involving  $s_{zz}^{(0)}$  in (77) which couple  $s_{zz}^{(0)}$  and the shear stress, and also due to the applied friction boundary condition. The dilemma is remedied in rolling (as it would be here also) by changing the boundary condition from a friction condition to a condition requiring the shear stress to equal its current yield value at points where the shear stress would exceed its yield value using a friction condition (see, for example, Alexander [15]). Changing the boundary condition amounts to replacing the shear stress term  $\mu\sigma_{\theta\theta}^{(0)}$  in (92) by the local value of the yield stress or flow stress in shear, say  $k = (\sqrt{3}/2)y(z)$ . That is, when solving (92) the shear stress term is taken to be equal to  $\mu\sigma_{\theta\theta}$  or  $k$  whichever is smaller.

Note also that within the context of the complete set of equations (76)–(78) it is not actually possible for  $s_{\rho z}^{(0)}$  to equal its current yield value because this would imply that  $s_{zz}^{(0)}$  vanishes and this is not possible in light of the flow-rule (78). From equation (78) we see that the shear strain rate term  $\mu\dot{s}_{\rho z}^{(0)}/\tau s_{zz}^{(0)}$  on the right hand side prohibits  $s_{zz}^{(0)}$  from vanishing over any finite interval since this would result in infinite hardening (such an occurrence, of course, would also violate the near slug-flow requirement because it would imply large transverse velocity variations, see (62)). Consequently, although changing the boundary condition in the Orowan-type inhomogeneous theory generally allows calculations to be completed to larger values of  $\mu$  than would be possible otherwise, the rigorous basis for this step is questionable and it can only be viewed as a model. The entire approximation discussed above is clearly ad hoc in nature and any results obtained from it must be used with a great deal of caution. Based on this only a limited number of examples were examined using this approximation. Note, however, that the equivalent approximation is used in rolling analysis quite frequently.

Another popular approximation in rolling, which precedes the inhomogeneous theory of Orowan discussed above and also has an analogy in conical extrusion, is the homogeneous theory originally due to Von Kármán [16]. This case is similar to that described above and can be obtained from the present development by omitting all shear effects on  $s_{zz}^{(0)}$ , i.e.,  $s_{zz}^{(0)}$  is assumed to be given by its value in homogeneous compression. In place of (90) we simply have  $s_{zz}^{(0)} = y(z)$  (or equivalently equation (84)) and this is equivalent to

taking  $\omega(a) = 1/2$  ( $a = 0$ ) in equation (92). This approximation is, of course, identical to the solution for homogeneous compression discussed in section (a) above. In fact, equation (92) with  $\omega(a) = 1/2$  is easily transformed into equation (76) where  $s_{zz}^{(0)}$  is given by its result for homogeneous compression (84). From the present development we now see that Von Karman's homogeneous approximation represents a rational limit of the full equations, i.e.,  $\mu/\tau \ll 1$ , whereas Orowan's inhomogeneous theory represents an approximate model.

(d) *Examples*

Results for four examples which summarize the overall behavior of the solution are now presented. In each case the parameters in the work-hardening expression (7) were taken to be:  $n = 10$  and  $\epsilon_0 = 0.02$ . These values are representative of mild steel, although, changing them to more precisely fit a specific material behavior does not alter the qualitative character of the results to be discussed here. We limit our attention to conical extruders and the die radius is prescribed by  $\hat{h}(z) = \hat{h}_0[1 - r(\hat{z}/L)]$  where  $\hat{h}_0$  is the entrance die radius and  $r$  is the radius reduction. The first three examples, examples I, II and III, correspond to a reduction in radius of 25% ( $r = 0.25$ ). In example I  $\delta = 0.05$  ( $\hat{h}_0/L = \delta/r = 0.2$ ), in example II  $\delta = 0.125$  ( $\hat{h}_0/L = 0.5$ ) and in example III  $\delta = 0.25$  ( $\hat{h}_0/L = 1.0$ ). These cases correspond to die wall slopes of about 3°, 7°, and 14°, respectively. The fourth example (example IV) is similar to example III except that it considers a rather large radius reduction of 50% ( $r = 0.5$ ). In example IV  $\delta = 0.25$  ( $\hat{h}_0/L = 0.5$ ) giving a die inclination angle of 14° which is the same as in example III. The values of the parameters for the four examples are summarized in Table 1. We are primarily interested in those cases for which there are significant shear stresses and therefore we have limited ourselves to rather small values of  $\delta$  as required (recall that we must have  $\delta\mu/\tau \ll 1$  and we are primarily interested in  $\mu/\tau = O(1)$ ). For these specific examples we find that the asymptotic theory fails to be valid for values of  $\mu$  greater than: 0.11 in the example I, 0.16 in example II, 0.20 in example III, and 0.10 in example IV. That is, above these values of the friction coefficient the theory fails to be valid because the velocity variations in the transverse plane become substantial and the magnitude of  $\beta v_z^{(1)}$  becomes comparable to  $v_z^{(0)}$ . This is consistent with the fact that above these values of  $\mu$  it became difficult to obtain a converged solution from the iterative scheme. In example I we present results for four values of the friction coefficient,  $\mu = 0.06, 0.08$  and  $0.11$ , in example II the values of friction coefficient considered are  $\mu = 0.08, 0.12$  and  $0.16$ , in example III we consider  $\mu = 0.14, 0.17$  and  $0.20$ , and in example IV we consider  $\mu = 0.08, 0.09$  and  $0.10$ .

Due to the greater slope of the die in examples III and IV the shear effect is generally greater for these examples. In addition, due to the large reduction in example IV, shear

Table 1. Parameter values for the four examples considered

| Example | Radius reduction | $\delta = \Delta h/L$<br>(Slope) | $\hat{h}_0/L$ |
|---------|------------------|----------------------------------|---------------|
| I       | 25%              | 0.05 (3°)                        | 0.20          |
| II      | 25%              | 0.125 (7°)                       | 0.50          |
| III     | 25%              | 0.250 (14°)                      | 1.00          |
| IV      | 50%              | 0.250 (14°)                      | 0.50          |

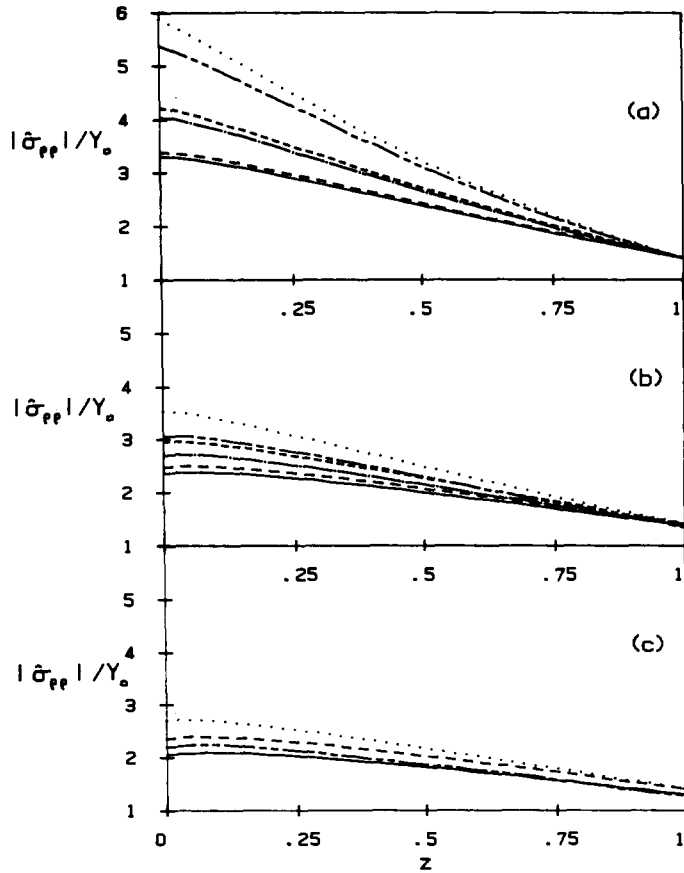


Fig. 2. Die pressure field ( $|\hat{\sigma}_{\theta\theta}|/Y_0$ ) versus  $z$  for examples I, II, III (25% reduction) shown in figures (a), (b) and (c) respectively. In each figure results are shown for the present theory and that predicted assuming homogeneous compression, i.e.,  $s_{zz}$  given by (84).

Figure (a),  $\delta = 0.05$ . Present theory:  $\mu = 0.06$ , —;  $\mu = 0.08$ , — · — · —;  $\mu = 0.11$ , — · — · — · —; homogeneous compression:  $\mu = 0.06$ , — · — · — · —;  $\mu = 0.08$ , — · — · — · —;  $\mu = 0.11$ , . . . .

Figure (b),  $\delta = 0.125$ . Present theory:  $\mu = 0.08$ , —;  $\mu = 0.12$ , — · — · —;  $\mu = 0.16$ , — · — · — · —; homogeneous compression:  $\mu = 0.08$ , — · — · — · —;  $\mu = 0.12$ , — · — · — · —;  $\mu = 0.16$ , . . . .

Figure (c),  $\delta = 0.25$ . Present theory:  $\mu = 0.14$ , —;  $\mu = 0.20$ , — · — · — · —; homogeneous compression:  $\mu = 0.14$ , — · — · — · —;  $\mu = 0.20$ , . . . .

effects become significant at smaller values of the friction coefficient. For example, in example III there is a 18% velocity variation from centerline to die wall at the entrance when  $\mu = 0.20$ , but in example IV a variation of this magnitude occurs at a much smaller value of  $\mu$ , namely, when  $\mu = 0.1$  (note that III and IV have the same slope parameter  $\delta = 0.25$ ).

In Fig. 2 the die pressure (i.e., the normal stress on the die walls) normalized by the yield stress  $Y_0$ , i.e.,  $|\hat{\sigma}_{\theta\theta}|/Y_0 = |\sigma_{\theta\theta}^{(0)}|/\tau$ , is plotted versus axial position  $z$  for  $\mu = 0.06, 0.08$  and  $0.11$  in example I, for  $\mu = 0.08, 0.12$  and  $0.16$  in example II, and for  $\mu = 0.14, 0.17$  and  $0.20$  in example III. Note that for the relatively small slopes being considered  $|\hat{\sigma}_{\theta\theta}|$  is, to leading order, equal to the normal stress on the die walls. Also shown in Fig. 2 are the corresponding pressure distributions predicted for the same values of  $\mu$  assuming that  $s_{zz}^{(0)}$  is given by the result for homogeneous compression, i.e.,  $\sigma_{\theta\theta}^{(0)}$  computed from (81) using  $s_{zz}^{(0)}$  given by (84) for homogenous compression. The pressure magnitude is generally greater in Fig. 2a than

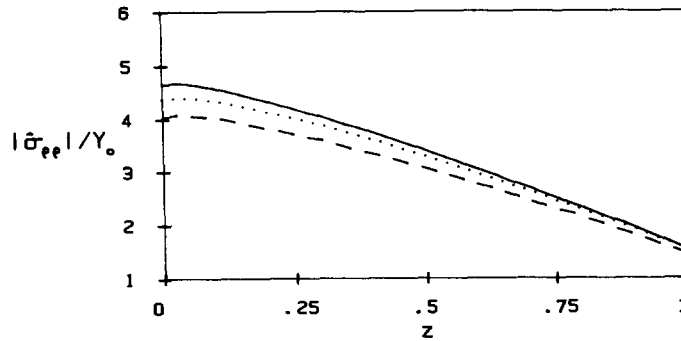


Fig. 3. Die pressure field ( $|\hat{\sigma}_{ee}|/Y_0$ ) versus  $z$  for example IV (50% reduction,  $\delta = 0.25$ ) with  $\mu = 0.10$ . Present theory: —; approximate inhomogeneous theory (Orowan approximation), . . . , and homogeneous compression — — —.

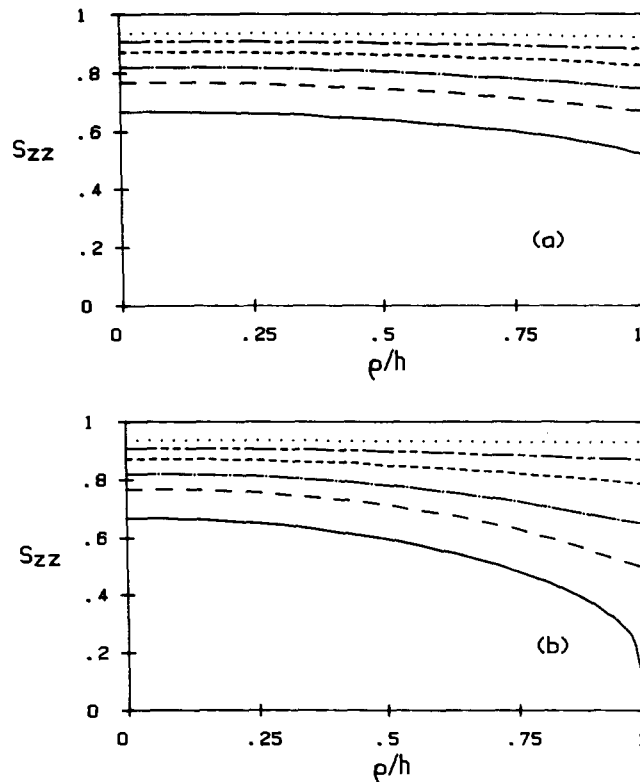


Fig. 4.  $s_{zz}$  versus  $\rho/h$  for example I ( $\delta = 0.05$  and a 25% reduction) with  $\mu = 0.08$  in figure (a) and  $\mu = 0.11$  in (b). Six axial locations are shown in each case:  $z = 0$ , —;  $z = 0.122$ , — — —;  $z = 0.268$ , — · — · —;  $z = 0.512$ , - - - -;  $z = 0.756$ , — · — · — · —;  $z = 1.0$ , . . . .

in 2b or 2c because  $\hat{h}_0/L$  is smallest in 2a and therefore the die is essentially longer for the same value of  $\hat{h}_0$ . For the longer die the net resistance to flow is greater and the pressures are correspondingly higher. Naturally as the friction coefficient increases the die pressure distributions generally increase, again due to the generally greater resistance. The pressure computed assuming an  $s_{zz}^{(0)}$  based on homogeneous compression and therefore neglecting

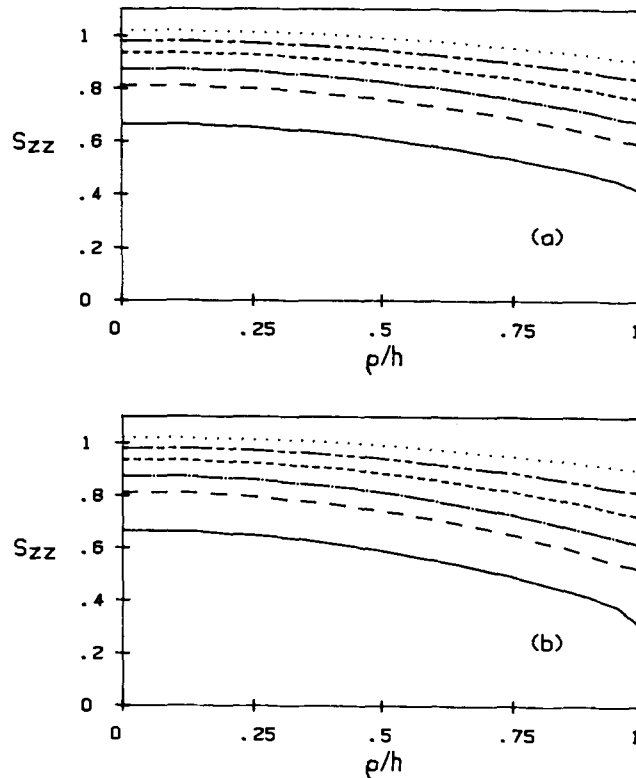


Fig. 5.  $s_{zz}$  versus  $\rho/h$  for example IV ( $\delta = 0.25$  and a 25% reduction) with  $\mu = 0.08$  in figure (a) and  $\mu = 0.10$  in (b). Six axial locations are shown in each case:  $z = 0$ , —;  $z = 0.122$ , — — —;  $z = 0.268$ , — · — · —;  $z = 0.512$ , - - -;  $z = 0.756$ , — · — · —;  $z = 1.0$ , . . . .

shear stresses is always over predicted; the worse case,  $\mu = 0.20$  in example III, shows a pressure difference of about 22%. In addition, as  $\mu$  increases the difference between the predictions from the present theory and that of homogeneous compression increases due to the greater role played by shear stresses. In Fig. 3 we compare the die pressure for example III computed from the present theory with the results computed based on the inhomogeneous theory analogous to Orowan's rolling theory (i.e., the solution to (92)) and to the case of homogeneous compression which was already shown in Fig. 2c. This figure is typical of what we find in all cases, namely, the inhomogeneous Orowan theory generally corrects for shear effects partially and gives better agreement for the pressure with the results of the more complete theory. However, due to its rather ad hoc nature, it is difficult to be certain when it will give reliable results. Lastly, since we have chosen to plot  $|\hat{\sigma}_{\theta\theta}|/Y_0$  in the figures, note that the value of  $\tau^{-1} = \sigma_0/Y_0$  is obtained from the value of  $|\hat{\sigma}_{\theta\theta}|/Y_0$  at  $z = 0$ .

The departure from a state of homogeneous deformation is shown in Figs. 4 and 5 where  $s_{zz}^{(0)}$  is plotted versus  $\rho/h$  for six axial locations. Fig. 4 corresponds to results for example I with  $\mu = 0.08$  in Fig. 4a and  $\mu = 0.11$  in Fig. 4b. Figure 5 corresponds to results for example IV and  $\mu = 0.08$  in Fig. 5a and  $\mu = 0.10$  in Fig. 5b. The value of  $s_{zz}^{(0)}$  along the centerline  $\rho/h = 0$  corresponds to the value for homogeneous compression and therefore the variation from homogeneous compression is easily seen. As expected, for small values of  $\mu$

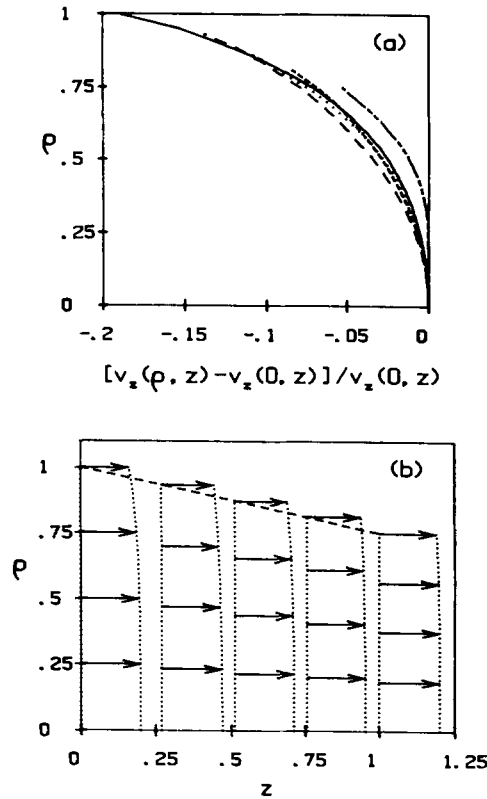


Fig. 6. Axial velocity variation from centerline to die wall for example III ( $\delta = 0.25$  and a 25% reduction) and  $\mu = 0.20$ . Figure (a) is a plot of  $[v_z(\rho, z) - v_z(0, z)]/v_z(0, z)$  versus  $\rho$  and (b) is a schematic of the axial velocity in the die shown as a dashed line. Note that in (b) the velocity at each axial location is normalized by the value at the centerline and therefore it appears that each location has the same centerline magnitude. The actual velocity is obtained by multiplying by  $v_z^{(0)}$ . Five axial positions are shown:  $z = 0$ , —;  $z = 0.268$ , — — —;  $z = 0.512$ , . . . ;  $z = 0.756$ , - - -;  $z = 1.0$ , — - - —.

the solution deviates the least from homogeneous compression. The variation of  $s_{zz}^{(0)}$  with respect to  $\rho$  is largest for the larger values of  $\mu$  in each case, particularly near the entrance  $z = 0$  where the pressures and therefore the shear stresses are largest. Close to the wall at the die entrance we see that  $s_{zz}^{(0)}$  can become rather small, indicating that there is considerable shearing. In fact, from Fig. 4b we see a case where  $s_{zz}^{(0)}$  is close to zero at the wall and therefore the shear stress is near its yield value. Note that  $s_{zz}^{(0)}$  adjusts and becomes nearly uniform as the material progresses from entrance to exit, i.e., as  $z$  increases. For the dies under consideration the variation of  $s_{zz}^{(0)}$  at the die exit was generally less than about 20%. Apparently the relatively rapid shearing deformation at the entrance has sufficient time to readjust itself so that by the time the material reaches the exit, the shearing motion has weakened noticeably. The longitudinal stress distributions shown are representative of the behavior seen in all of the cases examined.

In Fig. 6 the transverse variation of axial velocity  $v_z$  for example III is shown for five axial locations. In Fig. 6a we plot  $[v_z(\rho, z) - v_z(0, z)]/v_z(0, z)$  versus  $\rho$  for fixed values of  $z$  on an expanded scale to show the percent variation in the axial velocity from the centerline to the die wall. This result is readily obtained from the integration of (62). In Fig. 6b we show a

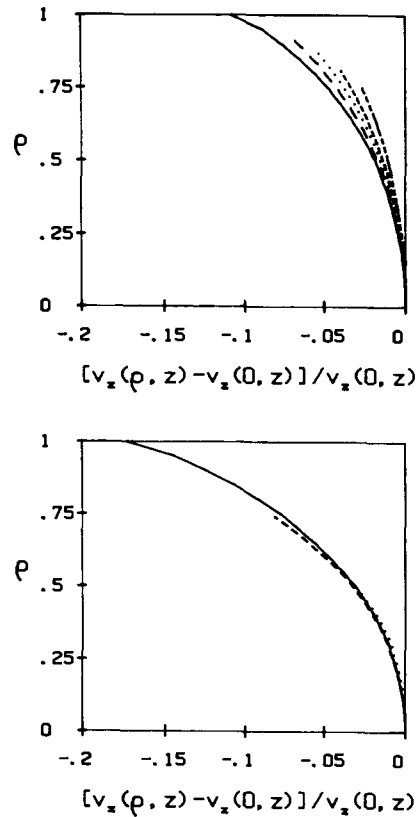


Fig. 7. Axial velocity variation from centerline to die wall, for example II with  $\mu = 0.16$  (top;  $\delta = 0.125$  and a 25% reduction) and example IV with  $\mu = 0.10$  (bottom;  $\delta = 0.25$  and a 50% reduction). Both examples have  $h_0/L = 0.5$ , but have different reductions and die slopes. Five axial positions are shown in the top figure:  $z = 0$ , —;  $z = 0.268$ , — — —;  $z = 0.512$ , . . . ;  $z = 0.756$ , - - -;  $z = 1.0$ , — — — — —. Three axial positions are shown in the bottom figure:  $z = 0$ , —;  $z = 0.512$ , — — —;  $z = 1.0$ , . . . .

sketch of the axial velocity in the die (the dotted line represents the die wall). In Fig. 6b note that the velocity at each axial location has been normalized by its centerline value and hence at each axial position the centerline value in the figure appears to have the same magnitude. The actual magnitude of the velocity is obtained by multiplying the results shown in Fig. 6b by  $h^2(0)/h(z)^2$ , the value of the velocity on the centerline. It was more convenient to plot the results as shown, due to the large increase in velocity which takes place from entrance to exit. In Fig. 6a we see that the axial velocity varies by about 18% from centerline to die wall at the entrance and by about 6% at the exit. Once again this indicates the tendency of the deformation to readjust to a near homogeneous deformation. In Fig. 7 we plot the velocity variation  $[v_z(\rho, z) - v_z(0, z)]/v_z(0, z)$  versus  $\rho$  for examples II and IV ( $h_0/L = 0.5$  in both cases). Naturally, example IV has a generally stronger shearing deformation at smaller values of the friction coefficient due to the greater reduction in that case, i.e., a 50% reduction in example IV versus 25% in example II.

In Figs. 8 and 9 we show the final deformation of an initially plane cross section which entered the die. That is, results for the axial displacement at the die exit versus  $\rho/h$  are shown for each of the four examples and a variety of friction coefficients. As expected, as  $\mu$  increases



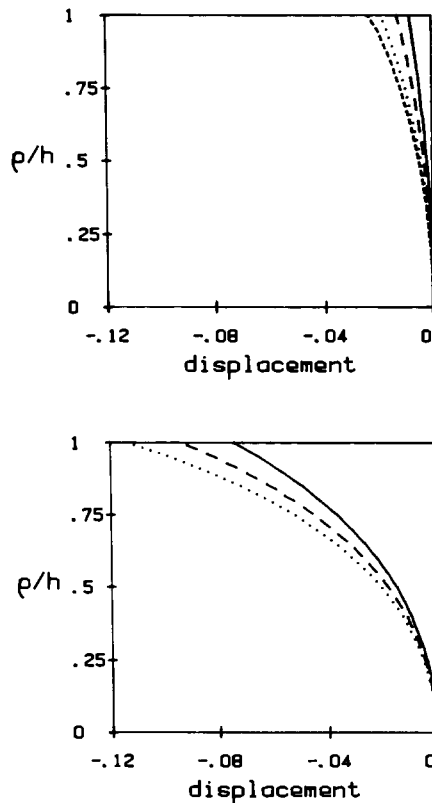


Fig. 8. Axial displacements at the exit versus  $q/h$  which show the net distortion of initially plane cross sections. Results are shown for examples I (top;  $r = 0.25$ ,  $h_0/L = 0.2$ ,  $\delta = 0.05$ ) and III (bottom;  $r = 0.25$ ,  $h_0/L = 1.0$ ,  $\delta = 0.25$ ). Both examples have a 25% reduction, but example III has a die wall slope five times greater than that of example I. A variety of friction coefficients are presented: top;  $\mu = 0.06$ , —;  $\mu = 0.08$ , — — —;  $\mu = 0.10$ , . . . ,  $\mu = 0.11$ , - - - , and bottom;  $\mu = 0.14$ , —;  $\mu = 0.17$ , — — —;  $\mu = 0.20$ , . . . .

the deformation from a plane section increases. In addition, the greatest die angle and largest reduction, example IV (Fig. 9), has the most severe distortion of a plane section and the most gentle die, example I, has the smallest final deformation. The displacements are very reminiscent of those calculated by Lee, et al. [10] using finite element methods. In Fig. 10 we show a typical comparison of the deformation predicted by the present theory and that predicted by the approximate inhomogeneous theory discussed in Section (c) (i.e., the Orowan-type model). The deformation is underestimated when the Orowan approximation is used and this is due to the fact that the shear stresses are always under predicted and therefore the transverse variation of the axial velocity determined from (62) is under predicted. A typical comparison of shear stress at the die wall predicted by the present theory (i.e., equation (77)) and the Orowan-type model is shown in Fig. 11. The large difference between the two is readily attributed to the omission of the terms involving  $s_{zz}^{(0)}$  in (77). In this case the parameter  $\delta\tau/\mu$  which affects the magnitude of these terms is approximately 0.57 ( $\mu = 0.20$ ,  $\delta = 0.25$  and  $\tau$  obtained from Fig. 2c is about  $1/2.2 = 0.45$ ), but the parameter  $\delta\mu/\tau$  establishing a “slug-like” flow is about 0.11 in this case. Generally as  $\delta$  decreases (milder slopes) we find that  $\tau$  decreases (note Figs. 2a–2c) and consequently the accuracy of the approximate Orowan-type theory improves because  $\delta\tau/\mu$  decreases.

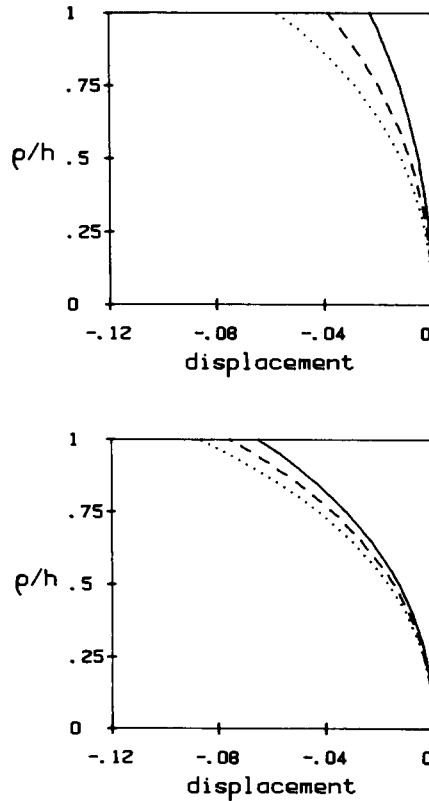


Fig. 9. Axial displacements at the exit versus  $q/h$  which show the net distortion of initially plane cross sections. Results are shown for examples II (top;  $r = 0.25, h_0/L = 0.5, \delta = 0.125$ ) and IV (bottom;  $r = 0.50, h_0/L = 0.5, \delta = 0.25$ ). Both examples have  $h_0/L = 0.5$ , but have different reductions. A variety of friction coefficients are presented: top;  $\mu = 0.08$ , —;  $\mu = 0.12$ , - - -;  $\mu = 0.16$ , . . . , and bottom;  $\mu = 0.08$ , —;  $\mu = 0.09$ , - - -;  $\mu = 0.10$ , . . . .

Lastly, in Fig. 12 we show a typical variation of flow stress as a function of axial position for three radial positions  $q/h = 0, 0.55$  and  $1.00$ , i.e., along the centerline, about midway to the die wall and along the die wall. The increase in the flow stress is naturally greatest along the wall due to the greater shearing there and the corresponding increase in hardening which is present there. Furthermore, since there is little difference between the results for  $q/h = 0$  and  $0.55$ , we find that the flow stress differs significantly from the value predicted by homogeneous compression only close to the wall. However, even along the wall the difference is not very severe. Also note that the difference is due to a more rapid hardening primarily near the entrance and thereafter the yield stress along the centerline and at the wall increase at a nearly equal rate.

### 5. Conclusions

We have investigated steady-state extrusion of an isotropic power-law hardening material when the axial velocity is nearly “slug-like”. The particular asymptotic limit considered,

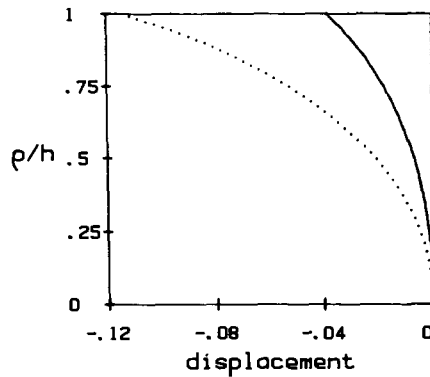


Fig. 10. Axial displacements at the exit versus  $q/h$  which show the net distortion of an initially plane cross section. Results are for example III ( $r = 0.25, \delta = 0.25$ ) with  $\mu = 0.20$ . Present theory:  $\dots$ ; approximate inhomogeneous theory (equivalent Orowan theory),  $\text{---}$ .

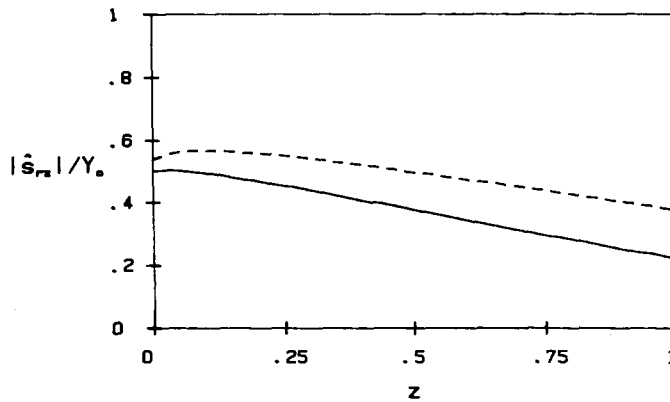


Fig. 11. Shear stress at the die wall  $q = h$  versus axial position  $z$  for example II ( $\delta = 0.125, r = 0.25$ ) with  $\mu = 0.16$ . Present theory  $\text{---}$ ; approximate inhomogeneous theory (equivalent Orowan theory),  $\text{- - -}$ .

namely  $\delta\mu/\tau < O(1)$ , generally has significant shear stresses and captures the first manifestations of inhomogeneous deformation. Transverse variations in the axial velocity are modest in size due to either a very small friction coefficient  $\mu$  or due to gentle die wall slopes,  $\delta < O(1)$ . When the friction coefficient is very small the stress field is that of homogeneous compression, i.e., negligible shear stress and longitudinal deviatoric stress given by equation (84). When the friction coefficient is on the order of 0.1 or greater, shear stresses become significant, i.e., on the order of the longitudinal deviatoric stress, and consequently a stress state which departs from homogeneous compression exists. A number of examples are considered and the typical departures which we find from homogeneous compression are discussed.

The present formulation also allowed us to develop a theory of extrusion which is analogous to the very popular inhomogeneous theory of sheet rolling developed by Orowan. The key assumptions of an "Orowan-type" inhomogeneous theory are shown to be somewhat ad hoc in nature and limitations of the theory are illustrated by the examples presented. For rough estimates, however, the extreme simplicity of the Orowan-type theory is very attractive.

The asymptotic theory developed only puts a dent in a small corner of a difficult problem, but it is believed that it contributes to our basic understanding of the subject. The theory also

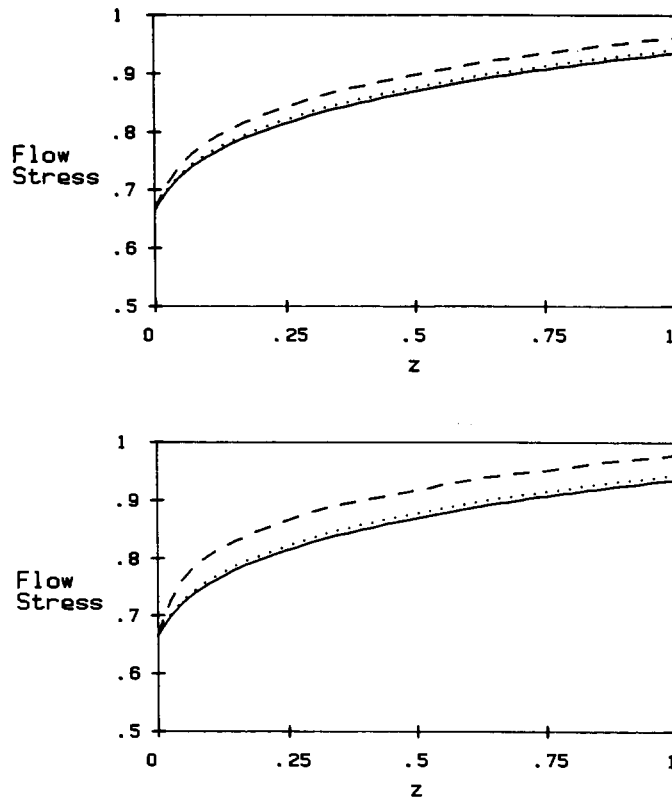


Fig. 12. Typical result for yield stress versus axial position  $z$  for three radial positions:  $q/h = 0.0$ , —;  $0.55$ , . . . ;  $1.0$ , — — —. The results shown are for example III and  $\mu = 0.14$  in the top figure and  $\mu = 0.20$  in the bottom figure.

offers a potentially useful simple special case against which much more elaborate numerical codes could be tested to assist in their verification.

### Acknowledgement

I would like to thank Robert M. McMeeking (UCSB) for the many useful comments which he made during early stages of this work and Robert P. Smet for reading the final manuscript. This project was supported, in part, by a grant from the National Science Foundation (MSM 85-13795).

### Appendix I

#### *Elastic entrance region*

Here we consider the solution in the elastic region at the entrance to the die. It is well-known that the elastic strains in this region are of order  $\alpha = Y_0/G$  and therefore very small. In this case the governing equations can be reduced to those of linear elasticity. In particular, since

the stress rate  $\dot{s}_{ij} \approx Ds_{ij}/D\hat{t}$  and  $\partial\hat{v}_i/\partial\hat{x}_j \approx (D/D\hat{t})(\partial\hat{u}_i/\partial\hat{x}_j)$ , where  $\hat{\mathbf{u}}$  is the displacement field and  $D/D\hat{t}$  the material or convective derivative, we can rewrite the dimensionless governing equations in the usual form for linear elasticity, i.e.,

$$e_{ij}^e - \frac{1}{3}e_{kk}^e\delta_{ij} \simeq \frac{1}{2}s_{ij}, \quad (I1)$$

$$e_{kk}^e \simeq \frac{1-2\nu}{2(1+\nu)}\frac{1}{\tau}\sigma_{kk}, \quad (I2)$$

where  $\frac{1}{2}(u_{i,j} + u_{j,i}) = \alpha e_{ij}^e$  and the presence of  $\alpha = Y_0/G$  in this expression is consistent with the nondimensional form of the equations being used (see (18)–(20)); note that we have normalized the strains as follows:  $e_{ij} = \hat{e}_{ij}^e/(Y_0/G)$ . Also note that the appearance of  $\tau = Y_0/\sigma_0$  in equation (I2) is related to the different scalings used for  $\sigma_{ij}$  and  $s_{ij}$  (see (I1) and (I2)), namely  $\sigma_{ij} = \hat{\sigma}_{ij}/\sigma_0$  and  $s_{ij} = \hat{s}_{ij}/Y_0$ . Furthermore, taking cylindrical coordinates and considering axisymmetric deformation these can be recast in the well known form

$$\frac{\partial u_\varrho}{\partial \varrho} = \alpha^* \{ \sigma_{\varrho\varrho} - \nu(\sigma_{\phi\phi} + \sigma_{zz}) \}, \quad (I3)$$

$$\frac{\partial u_z}{\partial z} = \alpha^* \{ \sigma_{zz} - \nu(\sigma_{\varrho\varrho} + \sigma_{\phi\phi}) \}, \quad (I4)$$

$$\frac{u_\varrho}{\varrho} = \alpha^* \{ \sigma_{\phi\phi} - \nu(\sigma_{\varrho\varrho} + \sigma_{zz}) \}, \quad (I5)$$

$$\frac{\partial u_z}{\partial \varrho} + \delta^2 \frac{\partial u_\varrho}{\partial z} = \delta \alpha s_{\varrho z}, \quad (I6)$$

where we define  $\alpha^* = \alpha/[2\tau(1+\nu)]$ . As before  $\varrho$  has been made dimensionless using  $\Delta h$  and  $z = \hat{z}/L$ . Similarly, the displacements have been made dimensionless as follows,

$$u_\varrho = \hat{u}_\varrho/\Delta h, \quad u_z = \hat{u}_z/L. \quad (I7)$$

Lastly, from (I3)–(I6) we see clearly that the elastic strains are of order  $\alpha$  (note  $\alpha^* = O(\alpha)$ ).

From (I6) we find that at leading order  $u_z \cong u_z(z)$ . Consequently,  $\partial^2 u_z/\partial\varrho\partial z = 0$  which from (I4) allows us to write

$$\frac{\partial}{\partial \varrho} \{ \sigma_{zz} - \nu(\sigma_{\varrho\varrho} + \sigma_{\phi\phi}) \} = 0. \quad (I8)$$

Now we can write

$$\frac{\partial u_\varrho}{\partial \varrho} - \frac{u_\varrho}{\varrho} = \varrho \frac{\partial}{\partial \varrho} \left( \frac{u_\varrho}{\varrho} \right) = \alpha^* \varrho \frac{\partial}{\partial \varrho} \{ \sigma_{\phi\phi} - \nu(\sigma_{\varrho\varrho} + \sigma_{zz}) \}, \quad (I9)$$

using (I 5). After substituting for  $\partial\sigma_{zz}/\partial\varrho$  obtained from (I 8) we find

$$\frac{\partial u_\varrho}{\partial\varrho} - \frac{u_\varrho}{\varrho} = \alpha^*(1 + \nu)\varrho \frac{\partial}{\partial\varrho} \{(1 - \nu)\sigma_{\phi\phi} - \nu\sigma_{\varrho\varrho}\}. \quad (\text{I } 10)$$

From the radial equilibrium equation (41a) we have, neglecting terms of  $O(\mu\delta)$ ,

$$\frac{\partial\sigma_{\varrho\varrho}}{\partial\varrho} = -\frac{\sigma_{\varrho\varrho} - \sigma_{\phi\phi}}{\varrho}, \quad (\text{I } 11)$$

and therefore substituting  $\partial\sigma_{\varrho\varrho}/\partial\varrho$  into the right side of (I 10) gives

$$\frac{\partial u_\varrho}{\partial\varrho} - \frac{u_\varrho}{\varrho} = \alpha^*(1 + \nu)\varrho \left\{ (1 - \nu) \frac{\partial\sigma_{\phi\phi}}{\partial\varrho} + \nu \frac{\sigma_{\varrho\varrho} - \sigma_{\phi\phi}}{\varrho} \right\}. \quad (\text{I } 12)$$

Alternatively, computing  $\partial u_\varrho/\partial\varrho - u_\varrho/\varrho$  directly from the difference between (I 3) and (I 5) we have

$$\frac{\partial u_\varrho}{\partial\varrho} - \frac{u_\varrho}{\varrho} = \alpha^*(1 + \nu)(\sigma_{\varrho\varrho} - \sigma_{\phi\phi}). \quad (\text{I } 13)$$

Equating (I 12) and (I 13) gives

$$\frac{\partial\sigma_{\phi\phi}}{\partial\varrho} = \frac{\sigma_{\varrho\varrho} - \sigma_{\phi\phi}}{\varrho},$$

which when substituted into the equilibrium equation (I 11) gives

$$\frac{\partial}{\partial\varrho} (\sigma_{\varrho\varrho} + \sigma_{\phi\phi}) = 0, \quad \sigma_{\varrho\varrho} + \sigma_{\phi\phi} = \text{function}(z). \quad (\text{I } 14)$$

Using this in (I 8) then gives,

$$\frac{\partial\sigma_{zz}}{\partial\varrho} = 0 \quad \text{or} \quad \sigma_{zz} = \sigma_{zz}(z). \quad (\text{I } 15)$$

Taking the sum of (I 3) and (I 5) we also have

$$\frac{\partial u_\varrho}{\partial\varrho} + \frac{u_\varrho}{\varrho} = \frac{1}{\varrho} \frac{\partial}{\partial\varrho} (\varrho u_\varrho) = \alpha^* \{(1 - \nu)(\sigma_{\varrho\varrho} + \sigma_{\phi\phi}) - 2\nu\sigma_{zz}\} \equiv F(z), \quad (\text{I } 16)$$

which, since the right-hand side is a function only of  $z$  (from (I 14) and (I 15)), we can integrate to find  $u_\varrho$ ,

$$u_\varrho = \frac{1}{2}F(z)\varrho, \quad (\text{I } 17)$$

where we have applied the symmetry condition  $u_\rho(0, z) = 0$ . The function  $F(z)$  defined in (I 16) and appearing in (I 17) is determined by the boundary condition on the radial displacement at the die faces  $\rho = h(z)$ , i.e.,

$$\hat{u}_\rho = \hat{h}(z) - \hat{h}(0),$$

or in dimensionless terms,

$$u_\rho = h(z) - h_0,$$

where  $h_0 = \hat{h}(0)/\Delta h$ , giving

$$F(z) = 2[h(z) - h_0]/h(z). \tag{I 18}$$

From the radial displacement field we now see that  $u_\rho/\rho = \partial u_\rho/\partial \rho$  and therefore returning to (I 13) we see that

$$\alpha^*(1 + \nu)(\sigma_{\rho\rho} - \sigma_{\phi\phi}) = 0, \tag{I 19}$$

$$\sigma_{\rho\rho} = \sigma_{\phi\phi},$$

and consequently,

$$s_{\rho\rho} = s_{\phi\phi}. \tag{I 20}$$

Since we found  $\sigma_{zz} = \sigma_{zz}(z)$  the shear stress is determined from the axial equilibrium equation (41b) by integration as,

$$\tilde{s}_{\rho z} = -\frac{\delta}{\mu} \frac{d\sigma_{zz}}{dz} \frac{\rho}{2}. \tag{I 21}$$

where, by symmetry, we have applied  $\tilde{s}_{\rho z}(0, z) = 0$ . In addition, from the definition of  $F(z)$  in equation (I 16) we can also express  $\sigma_{\rho\rho}$  in terms of  $\sigma_{zz}$  using (I 19) as

$$\sigma_{\rho\rho} = \frac{1}{1 - \nu} \left\{ \nu \sigma_{zz} + \frac{1}{2\alpha^*} F(z) \right\}, \quad \text{where } F(z) = 2(h - h_0)/h. \tag{I 22}$$

Finally,  $\sigma_{zz}$  is determined from the friction condition (42) at the die faces using the expressions for  $\tilde{s}_{\rho z}$  and  $\sigma_{\rho\rho}$  obtained above, i.e.,

$$\sigma_{\rho\rho} - \tilde{s}_{\rho z} - \frac{\delta}{\mu} h'(\sigma_{\rho\rho} - \sigma_{zz}) = 0 \quad \text{on } \rho = h(z),$$

$$\frac{d\sigma_{zz}}{dz} + 2 \left[ \frac{\nu\mu/\delta + h'(1 - 2\nu)}{1 - \nu} \right] \frac{\sigma_{zz}}{h(z)} = 2 \frac{\mu/\delta - h'}{\alpha^*(1 - \nu)} \left( \frac{h_0 - h}{h^2} \right), \tag{I 23}$$

which is a differential equation for the axial stress. If we are considering a configuration as shown in Fig. 1, then prior to when the material enters the die, i.e., for  $z < 0$ , the material has a constant radius and shear free surfaces. Consequently, it is appropriate outside the die entrance to take  $h' = 0$  and  $\mu = 0$  for  $z < 0$  giving  $d\sigma_{zz}/dz = 0$  or  $\sigma_{zz} = \text{constant}$  as expected under these circumstances. The boundary condition to be used when solving (I 23) will be discussed shortly. Once (I 23) is solved for  $\sigma_{zz}$ , the stress field in the elastic zone is known and direct integration of (I 4) determines  $u_z(z)$ .

The only unfinished task is to determine the elastic-plastic boundary  $z^p = z(\varrho)$ . This is obtained from the yield criterion

$$\frac{3}{4}s_{zz}^2 + s_{\varrho z}^2 = \frac{1}{3}, \quad (\text{I 24})$$

recalling that  $s_{\varrho z} = (\mu/\tau)\tilde{s}_{\varrho z}$ . Substituting for  $d\sigma_{zz}/dz$  obtained from (I 23) in the expression (I 21) for  $\tilde{s}_{\varrho z}$  and evaluating  $s_{zz} = (2/3\tau)(\sigma_{zz} - \sigma_{\varrho\varrho})$  using (I 22) we have

$$s_{\varrho z} = \frac{\varrho}{h} \left\{ a\sigma_{zz} + \frac{b}{\alpha^*} F(z) \right\}. \quad (\text{I 25})$$

where,

$$a = [v\mu + \delta h'(1 - 2v)]/[\tau(1 - v)], \quad b = [\mu - \delta h']/[2\tau(1 - v)],$$

and

$$s_{zz} = f\sigma_{zz} + \frac{1}{\alpha^*g} F(z), \quad (\text{I 26})$$

where

$$f = \frac{2}{3\tau}(1 - 2v)/(1 - v), \quad g = 3\tau(v - 1).$$

The yield criterion equation (I 24) can now be written as

$$\left( \frac{\alpha^* s_{zz}}{\sigma_{zz}} \right)^2 + \frac{4}{3} \left( \frac{\alpha^* s_{\varrho z}}{\sigma_{zz}} \right)^2 = \left( \frac{2\alpha^*}{\sigma_{zz}} \right)^2.$$

Defining  $G(z) = -F(z)/g\sigma_{zz} = 2(h_0 - h)/hg\sigma_{zz}$  and using (I 25) and (I 26) we obtain

$$(G - \alpha^* f)^2 + \frac{4}{3} \left( c_1 \frac{\varrho}{h} \right)^2 (G - \alpha^* c_2)^2 = \alpha^{*2} c_3, \quad (\text{I 27})$$

where

$$f = \frac{2(1 - 2v)}{3\tau(1 - v)},$$



$$c_1 = bg = -\frac{3}{2}(\mu - \delta h'), \tag{I28}$$

$$c_2 = a/bg = -\frac{v\mu + \delta h'(1 - 2v)}{6\tau(\mu - \delta h')(1 - v)},$$

$$c_3 = 4/\sigma_{zz}^2.$$

Now recall that  $\alpha^*$  introduced in (I 3)–(I 6) is equal to  $\alpha/[2\tau(1 + v)]$  and that it is very small since  $\alpha = Y_0/G$  is small. Consequently, in order for the sum of the squares in (I 27) to be of  $O(\alpha^2)$ , clearly  $G = 2(h_0 - h)/gh\sigma_{zz} = O(\alpha)$  which implies that  $h(z) = h_0(1 - rz) = h_0 + O(\alpha)$ . That is, the elastic–plastic boundary in the present approximation is only a small perturbation from the entrance plane of the die  $z = 0$ . Consequently, within the accuracy of the present approximation the boundary conditions on the plastic region can be applied at  $z = 0$ . This of course is a great simplification. The shape of the elastic–plastic boundary predicted from (I 27) at higher order will be discussed shortly.

It is now important to note the following character of the solution. The elastic loading region is coupled to the region of plastic deformation through the stress condition required to solve (I 23) for  $\sigma_{zz}$  in the elastic region. In contrast, since we have determined the elastic–plastic boundary to be  $z \approx 0$ , the deformation in the plastically deforming region can be solved (equations (76)–(78)) independent of the solution in the elastic region, at least to leading order.

Returning to the boundary condition on  $\sigma_{zz}(z)$  in the elastic region, the appropriate condition on  $\sigma_{zz}(z)$  is that the axial stress at the elastic–plastic boundary be continuous. Now, in the plastic region we have  $\sigma_{zz}^{(0)} = \sigma_{\varrho\varrho}^{(0)} + \frac{3}{2}\tau s_{zz}^{(0)}$  and, although  $\sigma_{\varrho\varrho}^{(0)}$  is a function only of  $z$  in the plastic region,  $s_{zz}^{(0)}$  is in general a function of  $\varrho$  and  $z$ . Consequently, the axial stress continuity condition can be satisfied approximately by requiring that the net axial force be continuous. To leading order this condition may be written as

$$\sigma_{zz}^{\text{elastic}} = 2 \int_0^1 \sigma_{zz}^{\text{plastic}}(\varrho, 0) \varrho d\varrho = \sigma_{\varrho\varrho}^{(0)}(0) + 3\tau \int_0^1 \varrho s_{zz}^{(0)}(\varrho, 0) d\varrho. \tag{I29}$$

The inability to satisfy the boundary condition exactly implies that there is generally a small region of nonuniformity in the elastic zone and an inner solution in this region is required to satisfy the stress condition exactly. An exception to this occurs if  $\mu$  is sufficiently small, in which case  $s_{zz}^{(0)}$  is a function only of  $z$  (i.e., homogeneous compression) and the stress boundary condition can be met exactly. Although we have not pursued the solution in this inner region (in fact, obtaining an analytic description is probably hopeless), it would likely be one for which the axial and radial derivatives are of the same order of magnitude. As already mentioned, however, the elastic solution, including a possible inner elastic region, has no effect on the leading-order solution in the plastically deforming region determined from (76)–(78). Lastly, note also that condition (I 29) is very similar to the approximate net-force condition imposed at the exit to the die (equation (29)). Namely, at the exit a small region of nonuniformity also exists, but we apply a condition on the net axial force.

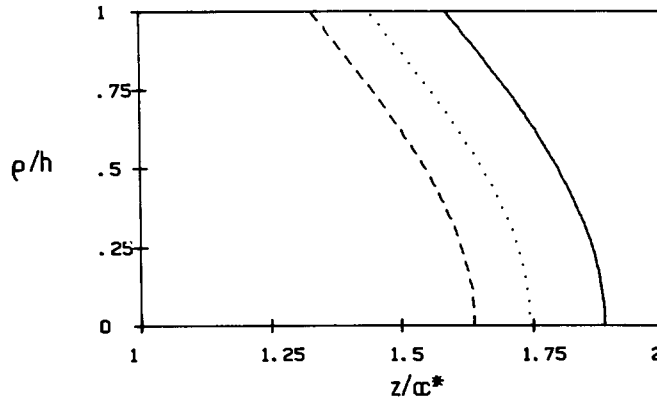


Fig. A1. Axial position of elastic-plastic boundary versus  $\rho/h$  for example II ( $\delta = 0.125, r = 0.25$ ). Note that  $z$  is normalized by  $\alpha^*$  where typically  $\alpha^* = O(10^{-3})$ .  $\mu = 0.08$ , —;  $\mu = 0.12$ , ...;  $\mu = 0.16$ , ---.

In any case, for any practical purposes the solution of (I23) using the condition (I29) should give adequate results. For the situation shown in Figure 1 (see the discussion following (I23)) the leading-order solution to (I23) outside the die, i.e.,  $z < 0$ , is  $\sigma_{zz} = \text{constant}$ . Since we found that the elastic region extends within the die by an amount of order  $\alpha$ , then it is appropriate to introduce into (I23)  $z = \alpha Z$  ( $Z = O(1)$ ) for this region and expand  $\sigma_{zz}$  in terms of  $\alpha$ . Naturally, the leading-order solution is once again  $\sigma_{zz} = \text{constant}$  and the constant value is found from the boundary condition (I29) at the elastic-plastic boundary once the solution to (76)–(78) has been obtained. This, of course, also sets the value of the  $\sigma_{zz}$  outside the die for  $z < 0$ . If desired, order  $\alpha$  modifications to the stress can be computed for the small region inside the die, but these are likely to be of little practical value since  $\alpha = O(10^{-3})$ . Note that the leading-order constant value of  $\sigma_{zz}$  obtained from (I29) can now be used in (I27) and the shape of the elastic-plastic boundary can be determined.

We can now return to equation (I27) and evaluate the shape of the elastic-plastic boundary for a typical example. In the case of a conical extruder  $h(z) = h_0(1 - rz)$  which gives  $G(z) = 2(h_0 - h)/hg\sigma_{zz} = 2rz/[(1 - rz)3\tau(v - 1)\sigma_{zz}]$ . Furthermore we let  $z = \alpha^*Z$  and therefore  $G(z) \simeq 2\alpha^*rZ/3\tau\sigma_{zz}(v - 1)$  and (I27) becomes

$$(c_0Z - f)^2 + \frac{4}{3} \left( c_1 \frac{\rho}{h} \right)^2 (c_0Z - c_2)^2 = c_3$$

where  $c_0 = 2r/3\tau\sigma_{zz}(v - 1)$ . As a typical case consider example II ( $\delta = 0.125, r = 0.25$ ) and take Poisson's ratio  $\nu = 0.3$ . When  $\mu = 0.08$  we find  $\tau = 0.424$  and  $\sigma_{zz} = -0.604$  (note  $\sigma_{zz}$  appears in the coefficients  $c_0$  and  $c_3$  and is obtained from (I29)), when  $\mu = 0.12$  we find  $\tau = 0.369$  and  $\sigma_{zz} = -0.680$ , and when  $\mu = 0.16$  we find  $\tau = 0.325$  and  $\sigma_{zz} = -0.751$ . In Fig. A1 we plot  $Z = z/\alpha^*$  versus  $\rho/h$  for these three values of the friction coefficient. As expected, as  $\mu$  increases the elastic-plastic boundary moves closer to the entrance of the die. Also note that the elastic-plastic boundary is always closer to the entrance at the die wall due to the larger shearing occurring there.

## References

1. I.F. Collins and B.K. Williams, Slipline fields for axisymmetric tube drawing, *Int. J. Mech. Sci.* 27 (1985) 225–233.
2. J.L. Chenot, L. Felgeres, B. Lavarenne and J. Salencon, A numerical application of the slip line field method to extrusion through conical dies, *Int. J. Engng. Sci.* 16 (1978) 263–273.
3. O. Richmond and H.L. Morrison, Application of a perturbation technique based on the method of characteristics to axisymmetric plasticity, *J. Appl. Mech.* 35 (1968) 117–122.
4. B. Avitzur, Analysis of wire drawing and extrusion through conical dies of small cone angle, *J. Eng. Ind.* 85 (1963) 89–96.
5. B. Avitzur, Analysis of wire drawing and extrusion through conical dies of large cone angle, *J. Eng. Ind.* 86 (1964) 305–316.
6. B. Avitzur, Strain-hardening and strain-rate effects in plastic flow through conical converging dies, *J. Eng. Ind.* 89 (1967) 556–562.
7. B. Avitzur, Flow through conical converging dies with hydrodynamic lubrication treated as an adiabatic process. In: S.A. Tobias (ed) *17th Int. Machine Tool Design & Res. Conf.*, Birmingham (1976) 445–451.
8. K. Osakada and Y. Niimi, A study on radial flow field for extrusion through conical dies, *Int. J. Mech. Sci.* 17 (1975) 241–254.
9. E.H. Lee, R.L. Mallet and W.H. Yang, Stress and deformation analysis of the metal extrusion process, *Computer Methods in Appl. Mech. and Eng.* 10 (1977) 339–353.
10. E.H. Lee, R.L. Mallett and R.M. McMeeking, Stress and deformation analysis of metal forming processes, R.F. Jones, H. Armen and J.T. Fong (eds) *Numer. Modeling in Manufacturing Processes*, ASME Winter Annual Meeting, Atlanta, GA (1977) 19–33.
11. S. Kobayashi, Rigid-plastic finite element analysis of axisymmetric metal forming processes, R.F. Jones, H. Armen and J.T. Fong (eds) *Numer. Modeling in Manufacturing Processes*, ASME Winter Annual Meeting, Atlanta, GA (1977) 49–65.
12. E. Orowan, The calculation of roll pressure in hot and cold flat rolling, *Proc. Instn. Mech. Engrs.* 150 (1943) 140–167.
13. L. Prandtl, Anwendungsbeispiele zu einen Henckyschen Satz über das plastische Gleichgewicht, *Z. angew. Math. Mech.* 3 (1923) 401.
14. R. Venter and A. Abd-Rabbo, Modelling of the rolling process-I: Inhomogeneous deformation model, *Int. J. Mech. Sci.* 22 (1980) 83–92.
15. J.M. Alexander, On the theory of rolling, *Proc. Roy. Soc. London A* 326 (1972) 535–563.
16. T. von Kármán, Beitrag zur Theorie des Walzvorganges, *Z. angew. Math. Mech.* 5 (1925) 139–141.